Table 2. Confirmation and quantification by 2-color multiplex PCR analysis of fetal cell-free Y chromosome sequences (*SRY* and DYS14) in the serum of pregnant monkeys

Week of gestation	Animal ID	Absolute quantification (no. of copies/mL serum)		Phenotype of newborn
		SRY	DYS14	
5	1219105063	111	3656	male
	1219202035	31	1078	male
	1219302022[a]	48	859	male
	1219403039	ND	ND	female
	1219407112	ND	ND	female
	1219408142[a]	ND	ND	female
	1219505076[a]	ND	ND	female
	1219608115	170	1,416	male
	1219612175	ND	ND	female
	1310006041[a]	32	341	male
	1310010102	43	1231	male
	1310107066[a]	112	591	male
	1310209114	102	1063	male
	1310703030	100	3900	male
	1319709070	35	3087	male
	1319908059	44	4750	male
	Overall mean ± 1 SD	75.3 ± 45.9	1997.5 ± 1542.6	
12	1210006038	ND	ND	female
	1210010060	ND	ND	female
	1210012077	417	10,656	male
	1219302022[a]	834	11,813	male
	1219408142[a]	ND	ND	female
	1219505062	1343	23,125	male
	1219505076[a]	ND	ND	female
	1219706059	ND	ND	female
	1219809032	3,531	15,938	male
	1219909061	ND	ND	female
	1310005037	ND	ND	female
	1310006041[a]	1239	14,621	male
	1310107066[a]	472	15,938	male
	1310204058	ND	ND	female
	1310209116	ND	ND	female
	1310402034	917	40,313	male
	1310605063	1153	13,531	male
	1310605067	1084	11,875	male
	1310608109	ND	ND	female
	1319810050	2716	69,375	male
	Overall mean ± 1 SD	1370.6 ± 990.8[b]	22,718.5 ± 18,590.6[c]	
22	1219302022[a]	1731	69,375	male
	1219408142[a]	ND	ND	female
	1219505076[a]	ND	ND	female
	1310003012	ND	ND	female
	1310005037	ND	ND	female
	1310006041[a]	2394	37,530	male
	1310103027	ND	ND	female
	1310107066[a]	2288	131,250	male
	1310203041	12,625	68,750	male
	1310204058	ND	ND	female
	1310205070	3687	17,438	male

Table 2. Continued

Week of gestation	Animal ID	Absolute quantification (no. of copies/mL serum)		Phenotype of newborn
		SRY	DYS14	
	1310209115	ND	ND	female
	1310409112	ND	ND	female
	1310506075	10,875	32,250	male
	1310507077	3988	37,625	male
	1319706035	2993	20,375	male
	1319708060	3463	129,375	male
	1319802003	3013	4175	male
	1319907039	ND	ND	female
	1319911092	ND	ND	female
	Overall mean ± 1 SD	4705.7 ± 3796.3	54,814.3 ± 44,794.2	

ND, none detected
Data are expressed as the mean number of copies of 3 replicate reactions according to the mean C_t value.
[a]Pregnant macaque (n = 5) used for the detection and quantification of fetal cell-free Y chromosome sequences (*SRY* and DYS14) during subsequent fetal development.
[b]Value significantly different from that at 5 wk ($P < 0.001$) and 22 wk ($P < 0.05$).
[c]Value significantly ($P < 0.05$) different from that at 5 wk.

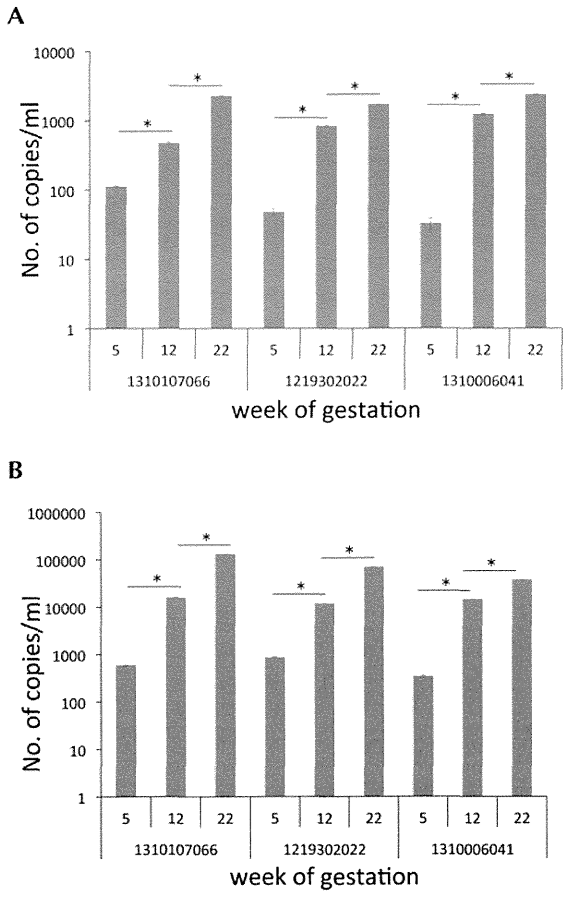

Figure 2. Comparison of the mean copy numbers of Y chromosome sequences (*SRY* and DYS14) in the maternal circulation of 5 pregnant monkeys continuously monitored during the 3 pregnancy stages. The real-time PCR quantification of copies of (A) *SRY* and (B) DYS14 sequences (mean from triplicate tests) were plotted against the time course of pregnancy. An increasing number of cell-free DNA copies in individual male-bearing pregnant monkeys (n = 3) were detected at 5, 12, and 22 wk of gestation. (A) *SRY* gene detection. (B) DYS14 detection. For both markers, the copy numbers in each animal were significantly different between weeks 5 and 12 and between weeks 12 and 22 (*, $P < 0.001$).

TSPY gene in nonhuman primates emphasize the difficulty in identifying an appropriate probe.[21] In humans, the copy number for DYS14 ranges from 50 to 200 copies per Y chromosome.[7] DYS14 reportedly is not an optimal marker for use in human quantification studies.[7]

We obtained no false-negative or false-positive results in the current study, highlighting the detection accuracy of this PCR method. By using specific probes, we were able to obtain a result in every case; indeed, targeting only a single gene in the Y chromosome might not provide an accurate result.[9] The fact that no false-negative results were found can be attributed to our use of a large quantity of DNA in the reaction. As another group has reported, contamination and false-negative results affect the reliability of the test.[17] A thorough understanding of the physiology of cell-free DNA in nonhuman primates, a large panel of biomarkers, and experiments related to fetal cell tracking could be helpful in many aspects related to the prenatal diagnosis and to increase the reliability of this test. Therefore, more studies need to be conducted regarding the availability of fetal DNA in both blood cells and plasma, and we have shown that nonhuman primates may be an important models to use. Although the application of this methodology has thus far been limited to sex determination in nonhuman primates, the recent advances toward genome editing research in nonhuman primate models of human genetic diseases may prompt investigators to adapt this method to monitor fetal genetic information at an early stage of pregnancy during the generation of strains with targeted gene modifications.

Our results confirm that our multiplex PCR technique, a noninvasive and effective method for detecting 2 target sequences from the *SRY* gene and DYS14 locus in a single reaction well by using cell-free fetal DNA in maternal blood, can be used successfully to determine fetal sex in cynomolgus monkeys. Furthermore, the results of the absolute quantification analysis demonstrated higher copy numbers of DYS14 compared with *SRY*, with a trend toward increased availability of fetal DNA in the maternal circulation during the later stages of pregnancy.

References

1. **Costa JM, Benachi A, Gautire E.** 2002. New strategy for prenatal diagnosis of X-linked disorders. N Engl J Med **346:**1502.
2. **Davoudi A, Seighalani R, Aleyasin SA, Tarang A, Radjabi R, Tahmoressi F.** 2011. The application of amplified TSPY and amelogenin genes from maternal plasma as a noninvasive bovine fetal DNA diagnosis. Eurasia J BioSci **5:**119–126.
3. **Devaney SA, Palomaki GE, Scott JA, Bianchi DW.** 2011. Noninvasive fetal sex determination using cell-free DNA: a systematic review and meta analysis. JAMA **306:**627–636.
4. **Finning KM, Chitty LS.** 2008. Noninvasive fetal sex determination: impact on clinical practice. Semin Fetal Neonatal Med **13:**69–75.
5. **Hill M, Barret AN, White H, Chitty LS.** 2012. Uses of cell-free fetal DNA in maternal circulation. Best Pract Res Clin Obstet Gynaecol **26:**639–654.
6. **Honda H, Miharu N, Ohashi Y.** 2002. Fetal gender determination in early pregnancy through qualitative and quantitative analysis of fetal DNA in maternal serum. Hum Genet **110:**75–79.
7. **Hromadnikova I, Benesova M, Zejskova L, Stehnova J, Doucha J, Sedlacek P, Dlouha K, Krofta L.** 2009. The effect of DYS14 copy number variations on extracellular fetal DNA quantification in maternal circulation. DNA Cell Biol **28:**351–358.
8. **Jimenez DF, Leapley AC, Lee CI, Ultsch M, Tarantal AF.** 2005. Fetal CD34+ cells in the maternal circulation and long-term microchimerism in rhesus monkeys (Macaca mulatta). Transplantation **79:**142–146.
9. **Jimenez DF, Tarantal AF.** 2003. Quantitative analysis of male fetal DNA in maternal serum of gravid rhesus monkeys (Macaca mulatta). Pediatr Res **53:**18–23.
10. **Jimenez DF, Tarantal AF.** 2003. Fetal gender determination in early first trimester pregnancies of rhesus monkeys (Macaca mulatta) by fluorescent PCR analysis of maternal serum. J Med Primatol **32:**315–319.
11. **Kadivar A, Hassanpour H, Mirshokraei P, Azari M, Korosh G, Karami A.** 2013. Detection and quantification of cell-free fetal DNA in ovine maternal plasma: use it to predict fetal sex. Theriogenology **79:**995–1000.
12. **Lo YM, Corbetta N, Chamberlain PF.** 1997. Presence of fetal DNA in maternal plasma and serum. Lancet **350:**485–487.
13. **Lo YM, Tein MS, Lau TK.** 1998. Quantitative analysis of fetal DNA in maternal plasma and serum. Am J Hum Genet **62:**768–775.
14. **Miura K, Higashijima A, Shimada T.** 2011. Clinical application of fetal sex determination using cell-free fetal DNA in pregnant carriers of X-linked genetic disorders. J Hum Genet **56:**296–299.
15. **Ostrer H, Wilson DI, Hanley NA.** 2006. Human embryo and early-fetus research. Clin Genet **70:**98–107.
16. **Sasaki E, Suemizu H, Shimada A, Hanazawa K, Oiwa R, Kamioka M, Tomioka I, Stomaru Y, Hirakawa R, Eto T, Shiozawa S, Maeda T, Ito M, Ito R, Kito C, Yagihashi C, Kawai K, Miyoshi H, Tanioka Y, Tamaoki N, Habu S, Okano H, Nomura T.** 2009. Generation of transgenic nonhuman primates with germline transmission. Nature **459:**523–527.
17. **Scheffer PG, Van der Schoot CE, Page-Christiaens GC.** 2010. Reliability of fetal sex determination using maternal plasma. Obstet Gynecol **115:**117–126.
18. **Tachdjian G, Frydman N, Audibert F, Ray P, Kerbrat V, Ernault P, Frydman R, Costa J.** 2002. Clinical application of fetal sex determination in maternal blood in a preimplantation genetic diagnosis center. Hum Reprod **17:**2183–2186.
19. **Treff NR, Tao X, Su J.** 2011. Tracking embryo implantation using cell-free fetal DNA enriched from maternal circulation at 9 weeks gestation. Mol Hum Reprod **17:**434–438.
20. **Wright CF, Burton H.** 2009. The use of cell-free fetal nucleic acids in maternal blood for noninvasive prenatal diagnosis. Hum Reprod Update **15:**139–151.
21. **Xue Y, Tyler-Smith C.** 2011. An exceptional gene: evolution of the *TSPY* gene family in human and other great apes. Genes **2:**36–47.
22. **Yang SH, Cheng PH, Banata H, Piotrowaska-Nitsche K, Yang JJ, Cheng EC, Snyder B, Larkin K, Liu J, Orkin J, Fang ZH, Smith Y, Bachevalier J, Zola SM, Li SH, Li XJ, Chan AW.** 2008. Towards a transgenic model of Huntington's diseases in a nonhuman primate. Nature **453:**921–924.
23. **Zimmermann B, El-Sheikhah A, Nicolaides K, Holzgreve W, Hahn S.** 2005. Optimized real-time quantitative PCR measurement of male fetal DNA in maternal plasma. Clin Chem **51:**1598–1604.

Journal of Reproduction and Development, Vol. 61, No 1, 2015

—Original Article—

Naïve-like conversion enhances the difference in innate *in vitro* differentiation capacity between rabbit ES cells and iPS cells

Kimiko HONSHO[1)]*, Michiko HIROSE[2)]*, Masanori HATORI[2)], Lubna YASMIN[3)], Haruna IZU[1)], Shogo MATOBA[2)#], Sumie TOGAYACHI[2)], Hiroyuki MIYOSHI[2)], Tadashi SANKAI[3)], Atsuo OGURA[2)] and Arata HONDA[1, 2)]

[1)]*Organization for Promotion of Tenure Track, University of Miyazaki, Miyazaki 889-1692, Japan*
[2)]*RIKEN BioResource Center, Ibaraki 305-0074, Japan*
[3)]*Tsukuba Primate Research Center, National Institute of Biomedical Innovation, Ibaraki 305-0843, Japan*
[#]*Present: Harvard Medical School, Boston, MA 02115, USA*

Abstract. Quality evaluation of pluripotent stem cells using appropriate animal models needs to be improved for human regenerative medicine. Previously, we demonstrated that although the *in vitro* neural differentiating capacity of rabbit induced pluripotent stem cells (iPSCs) can be mitigated by improving their baseline level of pluripotency, i.e., by converting them into the so-called "naïve-like" state, the effect after such conversion of rabbit embryonic stem cells (ESCs) remains to be elucidated. Here we found that naïve-like conversion enhanced the differences in innate *in vitro* differentiation capacity between ESCs and iPSCs. Naïve-like rabbit ESCs exhibited several features indicating pluripotency, including the capacity for teratoma formation. They differentiated into mature oligodendrocytes much more effectively (3.3–7.2 times) than naïve-like iPSCs. This suggests an inherent variation in differentiation potential *in vitro* among PSC lines. When naïve-like ESCs were injected into preimplantation rabbit embryos, although they contributed efficiently to forming the inner cell mass of blastocysts, no chimeric pups were obtained. Thus, *in vitro* neural differentiation following naïve-like conversion is a promising option for determining the quality of PSCs without the need to demonstrate chimeric contribution. These results provide an opportunity to evaluate which pluripotent stem cells or treatments are best suited for therapeutic use.

Key words: Embryonic stem cells (ESCs), Induced pluripotent stem cells (iPSCs), Naïve, Neural differentiation, Rabbit

(J. Reprod. Dev. 61: 13–19, 2015)

The generation of induced pluripotent stem cells (iPSCs) from human somatic cells has revolutionized the field of regenerative medicine, because use of these cells is expected to bypass the ethical concerns associated with the generation of human embryonic stem cells (ESCs) and issues of allogeneic immune rejection. However, the safety and efficacy of iPSC-derived cells must be tested rigorously using appropriate animal models and ESCs. We have successfully generated human-type (primed-state) ESCs and iPSCs from the rabbit [1, 2]. The laboratory rabbit (*Oryctolagus cuniculus*) is closer phylogenetically to primates than are rodents [3]. It has a short gestation period (31 days) and shows high fecundity. For these reasons, a number of research groups have long used the rabbit in biomedical research, and it has served as a model for several human diseases [4, 5]. Therefore, rabbit iPSCs have great potential as models for human iPSC research in many technical, medical and biological fields. They fulfill all the requirements for the acquisition of a fully reprogrammed genomic state, showing strong similarity to ESC counterparts that we have generated recently [2]. However, although the global gene expression profile of the rabbit iPSCs became closer to that of the rabbit ESCs as the number of cell passages increased, a slight but clear difference between the two types of cell lines remained [2]. *In vitro* neural differentiation assays have been used to evaluate whether the differences in their gene expression profiles reflect their differentiation capacities [6]. The *in vitro* neural differentiation capacities of rabbit iPSC lines can vary with the donor cell type, passage number and the target cell type into which they are induced to differentiate. Although the limited early neural differentiation capacity observed in the iPSC lines was improved by continuous passaging, more mature types of neural cells—such as oligodendrocytes—were generated only poorly, even from continuously passaged iPSCs [6].

On the other hand, several attempts to improve the differentiating potential of primed-state pluripotent stem cells (PSCs) have been successful by conversion of naïve-state cells [7–10]. PSCs exist in naïve or primed states, epitomized by mouse ESCs and the developmentally more advanced epiblastic stem cells (EpiSCs) [11]. Primed-state EpiSCs are considered to represent a more advanced "differentiated" state than that shown by naïve-state ESCs. Actually, unlike naïve-state ESCs, primed-state EpiSCs are highly inefficient in repopulating the inner cell mass (ICM) upon aggregation with or

Received: August 18, 2014
Accepted: September 17, 2014
Published online in J-STAGE: October 25, 2014

Correspondence: A Ogura (e-mail: ogura@rtc.riken.go.jp), A Honda (e-mail: a-honda@med.miyazaki-u.ac.jp)
*Honsho K and Hirose M contributed equally to this work.

injection into host blastocysts [12, 13]. Because human and rabbit PSCs so far have only assumed the primed state, their *in vitro* differentiation might be less effective than that of naïve-state PSCs. To overcome the limited neural differentiation capacity observed in primed-state iPSCs, we have established methods for conversion of primed-state iPSCs into a naïve-like state [6]. Indeed, naïve-like converted rabbit iPSCs effectively differentiated into the morphologically mature form of oligodendrocytes with ramified branches, which were not observed even when primed-state ESCs were induced to differentiate. Thus, the limited differentiation capacity of primed-state rabbit iPSCs was successfully improved to a similar or better extent than primed-state rabbit ESCs by naïve-like conversion [6].

Here we evaluated the naïve-like conversion of rabbit ESCs that have shown much better differentiating potential than naïve-like iPSCs. Several characteristics of naïve-like converted rabbit ESCs were assessed, including neural differentiation and the potential for chimeric pup production. Quality evaluation of rabbit PSCs will enable us to identify which type of cell is best suited for each type of human regenerative therapy.

Materials and Methods

Animals

All rabbits and mice were maintained and used for experiments in accordance with the guidelines for animal experimentation of University of Miyazaki, RIKEN Bioresource Center and Tsukuba Primate Research Center after approval by the responsible committees.

Cell culture

The method of establishment of rabbit PSCs used in this study was reported previously [2]. All of the PSCs were derived from Dutch belted rabbits. The PSCs can be divided roughly into three categories: ESCs, liver-derived iPSCs (iPS-L) and stomach-derived iPSCs (iPS-S). All rabbit iPSC lines (iPS-L1, -L2, -L3, -S1, -S2 and -S3) and ESC lines (rdES2-1, rdES4 and rdES6) were maintained by established methods [2]. Briefly, primed-state rabbit PSCs were plated onto mitomycin-C-treated mouse embryonic fibroblast layers at 37 C under 6% CO_2 in air. The culture medium consisted of 78% DMEM/Ham's F-12 supplemented with 20% knockout serum replacement (KSR) (Invitrogen Life Technologies), 1% nonessential amino acids, 0.1 mM β-mercaptoethanol and 8 ng/ml human recombinant basic fibroblast growth factor (bFGF) (Wako Pure Chemical Industries, Osaka, Japan).

Conversion of rabbits cells into the naïve-like state

To convert rabbit ESCs into a naïve-like state, the vector *CSII-EF-hOct3/4-IRES-Venus*, which drives the expression of human OCT3/4 and green fluorescent protein (GFP) under the control of the *EF1α* promoter, was introduced into rabbit ESCs and iPSCs and cultured as previously reported [6]. The culture medium consisted of 38% DMEM/Ham's F-12, 38% Neurobasal, 20% KSR, 1% N2 supplement, 2% B27 supplement, 1% nonessential amino acid (Invitrogen), 0.1 mM β-mercaptoethanol, 10 μM forskolin (Sigma-Aldrich, St. Louis, MO, USA), 5 μM kenpaullone (Calbiochem, San Diego, CA, USA), 3 μM CHIR990021 (Stemgent, Cambridge, MA, USA) and 0.1% human LIF (Wako). PSCs in a naïve-like state were passaged by incubating the cells with 0.25% trypsin/EDTA for 3 min at 37 C. After termination of the trypsin reaction by serum treatment, the cells were disaggregated mechanically into single cells. These were then resuspended and seeded into fresh culture plates.

RT-PCR analysis

Total RNA was isolated with ISOGEN (Nippon Gene, Toyama, Japan) from cells cultured under appropriate conditions. After DNase treatment to prevent contamination with genomic DNA, the first-strand cDNA was synthesized using a Takara RNA PCR kit (TaKaRa, Shiga, Japan). The synthesized cDNA was amplified by PCR using specific primers (Supplementary Table 1: online only) with a cycle program of 94 C for 3 min and 35 cycles of 94 C for 30 sec, 58 C for 30 sec and 72 C for 30 sec. For quantitative RT-PCR, a LightCycler 96 System (Roche Applied Science, Mannheim, Germany) was used to determine mRNA expression levels using FastStart Essential DNA Green Master (Roche Applied Science) with a program of 95 C for 10 min and 45 cycles of 95 C for 10sec, 60 C for 10 sec and 72 C for 10 sec.

Alkaline phosphatase staining

Rabbit naïve-like-state ES cells were stained using alkaline phosphatase detection kits (Sigma-Aldrich) according to the manufacturer's protocol.

Teratoma formation

To generate teratomas, $1–2 \times 10^6$ rabbit cells that had been converted to a naïve-like state were injected under the kidney capsules of 5–8-week-old SCID mice. At 4–8 weeks after transplantation, the teratomas were dissected out and fixed in paraformaldehyde. Paraffin wax sections were stained with hematoxylin and eosin.

In vitro oligodendrocyte differentiation

As previously reported [6], to induce oligodendrocyte differentiation, rabbit PSCs were digested with trypsin, suspended in embryoid body (EB) medium containing 78% DMEM/Ham's F-12 supplemented with 20% KSR, 1% nonessential amino acids, 50 units/ml penicillin, 50 μg/ml streptomycin, 0.1 mM β-mercaptoethanol, 1% N-2 supplement (Invitrogen), 4 μM all-*trans*-retinoic acid (Sigma-Aldrich) and 10 μM SB431542 (Tocris Bioscience, Bristol, UK). To achieve single EBs of a uniform size, 1,000 PSCs in a volume of 100 μl were dispensed into each well of low-cell-adhesion 96-well round bottom plates (Nunc, Thermo Fisher Scientific, Waltham, MA, USA), tapped gently and cultured at 37 C under 6% CO_2 in air. To obtain differentiated oligodendrocytes, six EBs were transferred to a Matrigel (BD Bioscience, Franklin Lakes, NJ, USA)-coated 4-well Multidish (Nunc) and allowed to attach to the bottoms of the wells. The medium was then changed from EB medium to neural differentiation medium (the same formulation as EB medium, with the addition of 10% KSR). After 10 days, the medium was changed from neural differentiation medium to the culture medium without retinoic acid or SB431542 but with 100 ng/ml Noggin (Wako). The cells were cultured for a further 20 days, with fresh medium added every day.

Immunohistochemistry

Marker protein expression was analyzed by fixing the differentiated cells that had attached to the bottoms of the culture plates in 4% paraformaldehyde for 30 min at room temperature. They were then washed three times (5 min each) with Tris-buffered saline containing 1% bovine serum albumin (BSA; wash buffer). To permeabilize the cells, the cells were treated with 0.1% Triton X-100 in wash buffer for 10 min and then incubated in blocking solution (10% normal donkey serum and 1% BSA in wash buffer) for 30 min. The following primary antibodies were used: anti-O1 (Santa Cruz Biotechnology, Santa Cruz, CA, USA) and anti-CNPase (Sigma-Aldrich). All antibodies were diluted with blocking solution and incubated with samples overnight at 4 C. The next day, the cells were washed three times with wash buffer and incubated with a secondary antibody at room temperature for 1 h. The cells were washed again and covered with 50% glycerol containing DAPI. The fluorescence signals were detected with a BZ-9000 Series All-in-One Fluorescence Microscope using the BZII image analysis software (Keyence, Osaka, Japan).

Quantification of neural differentiation

The immunopositive cells were quantified using a BZ-9000 Series All-in-One Fluorescence Microscope and the BZII image analysis (Keyence). Immunopositive signals for O1 and merged signals for O1 and CNPase were calculated per unit area of each well. The area of DAPI-labeled nuclei on each image was referred to as the total cell area per unit area of the well. The immunopositive area/DAPI area is indicated as the neural differentiation index. To evaluate the difference in differentiation capacity after naïve-like conversion between ESCs and iPSCs, the relative differentiation index of naïve-like ESCs was divided by that of naïve-like iPSCs.

Evaluation of the chimeric contribution

To evaluate whether the naïve-like ESCs could contribute to the embryos (rabbit or mouse) and pups (rabbit), naïve-like rdES2-1 cells were trypsinized to dissociate into single cells or small clumps. Recipient embryos were recovered from superovulated donor animals at the 8-cell stage following natural mating (for rabbit embryos) or after *in vitro* fertilization (for mouse embryos). Naïve-like rdES2-1 cells (n = 10–15) were injected into the perivitelline spaces of the 8-cell embryos using a Piezo-driven micromanipulator. Two days after injection, the contributions of the injected cells to the ICM of the blastocysts were determined by the presence of GFP fluorescence. From 2–3 h after injection, reconstructed rabbit 8-cell embryos were transferred into the oviducts of pseudopregnant female rabbits that had been treated with 100 IU human chorionic gonadotropin and finger vulval stimulation 3 days before transplantation. Chimerism of the 11.5-day (mouse) and 15.5-day (rabbit) post coitus (dpc) embryos and newborn pups was determined by the presence of GFP and a black coat color.

Statistical analysis

Mean values were compared using one-way analysis of variance using SPSS Statistics ver. 19. Where appropriate, the significance of differences between means was determined with Fisher's exact probability test; $P < 0.05$ was considered significant. All experiments were analyzed in triplicate at least.

Results

Naïve-like conversion of rabbit ES cells

To evaluate the efficacy of naïve-like conversion of rabbit ESCs, which are assumed to have a higher pluripotency than that of iPSCs, three ESC lines derived from Dutch belted rabbits were subjected to naïve-like conversion using a previously reported system [6]. To convert primed-state rabbit ESCs into a naïve-like state, a lentiviral vector was used to introduce a transgene driving *hOCT3/4-GFP* expression under the control of the *EF1α* promoter. Two or three passages after lentiviral transduction under the naïve-converting culture conditions, the colony morphology of rabbit ESCs changed to be almost indistinguishable from that of mouse ESCs, which showed transduced GFP expression and strong alkaline phosphatase activity (Fig. 1A) (Supplementary Fig. 1: online only). Although these cell lines can be maintained for more than 20 passages by single-cell dissociation with no obvious changes in their karyotype, genetically unmodified ESCs could not be maintained for longer than 2–3 passages even if the same culture conditions were used (data not shown). The mRNA expression levels of endogenous pluripotent stem cell marker genes, *OCT3/4*, *NANOG*, *KLF4*, *SOX2* and *cMYC* were maintained as naïve-like iPSCs after naïve-like conversion of rabbit ESCs (Fig. 1B). Moreover, increased expressions of the candidate genes, *KLF4* and *KLF5*, which are responsible for maintaining a naïve pluripotent state, were also confirmed by quantitative reverse transcription polymerase chain reaction (qRT-PCR) (Fig. 1C; see Supplementary methods). To evaluate the ability to differentiate into tissues representative of all three germ layers *in vivo*, naïve-like converted ESCs were transplanted into severe combined immunodeficient (SCID) mice. At 5–8 weeks after transplantation, teratomas were recovered and analyzed for the existence of three germ layers (Fig. 1D). These results confirmed the successful naïve-like conversion of rabbit ESCs.

In vitro differentiation of naïve-like ESCs into oligodendrocytes

We reported previously that ESCs and iPSCs showed almost the same *in vitro* ability to differentiate into neurons and astrocytes; however, the ability to differentiate into oligodendrocytes of the primed-state rabbit iPSCs was inferior to that of the primed ESCs. On the other hand, naïve-like iPSCs were able to differentiate into mature oligodendrocytes with dendrites, which was not observed even with the primed ESCs when differentiated [6]. It is now clear that *in vitro* differentiation into mature oligodendrocytes is a suitable indicator for assessing the quality of PSCs. Therefore, we used this system to evaluate the differentiation ability of ESCs and iPSCs before and after naïve-like conversion. The ability to differentiate *in vitro* into oligodendrocytes was evaluated among rabbit ESCs (primed and naïve-like states) and iPSCs (primed and naïve-like states; iPS-L and iPS-S cells). To detect oligodendrocytes, immunopositive signals for the anti-O1 antibody that recognizes immature oligodendrocytes and anti-O1 and anti-2′,3-cyclic nucleotide 3′-phosphodiesterase (CNPase) merged signals for detecting more mature types of oligodendrocytes were used (Fig. 2A and B) (Supplymentary Fig. 2A and B: online only). As reported previously [6], although the ability of iPS-S cells to differentiate into oligodendrocytes improved to be equivalent to that of primed-state ESCs by naïve-like conversion, iPS-L cells could not be improved sufficiently even after naïve-like conversion (Fig.

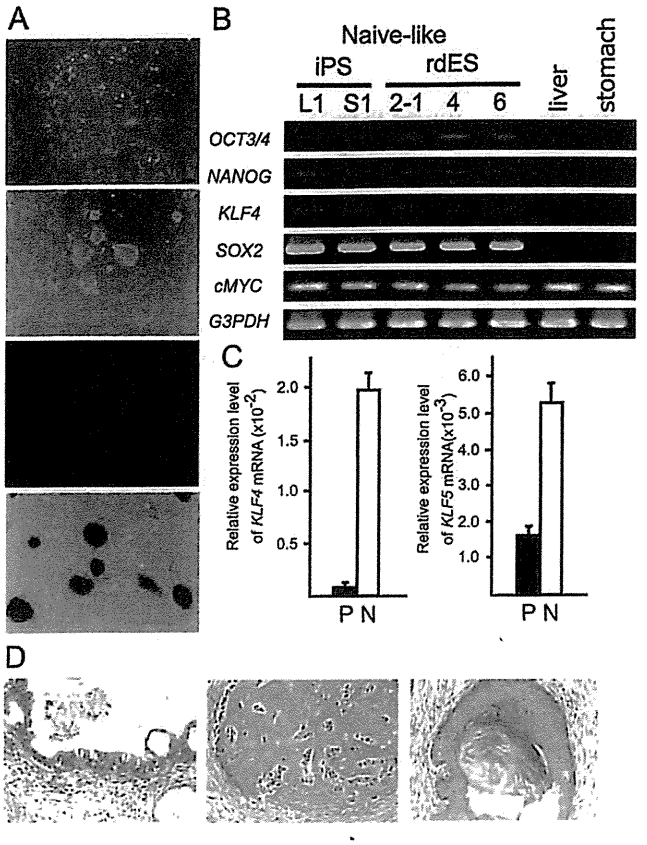

Fig. 1. Characterization of naïve-like rabbit ESCs. (A) Colony morphology of primed-state rabbit ESCs (rdES2-1 cell line) (top panel), naïve-like converted ESCs (upper middle panel), expressing hOCT3/4-IRES-GFP (lower middle panel) and demonstrating alkaline phosphatase activity (bottom panel). Scale bar = 200 μm. (B) RT-PCR analysis of pluripotent marker genes in naïve-like converted liver-derived iPS cells (iPS-L1), stomach-derived iPS cells (iPS-S1), ES cell lines (2-1, 4 and 6) and somatic cells (liver, stomach). (C) Quantitative real-time RT-PCR analysis of *KLF4* and *KLF5* expression in primed (closed bar) and naïve-like (open bar) ESCs (rdES2-1 cells). (D) Naïve-like converted ESCs were able to form teratomas containing tissues originating from the three primary germ layers: epithelium with Goblet cells (left panel; endoderm), bone (middle panel; mesoderm) and epidermis (right panel; ectoderm).

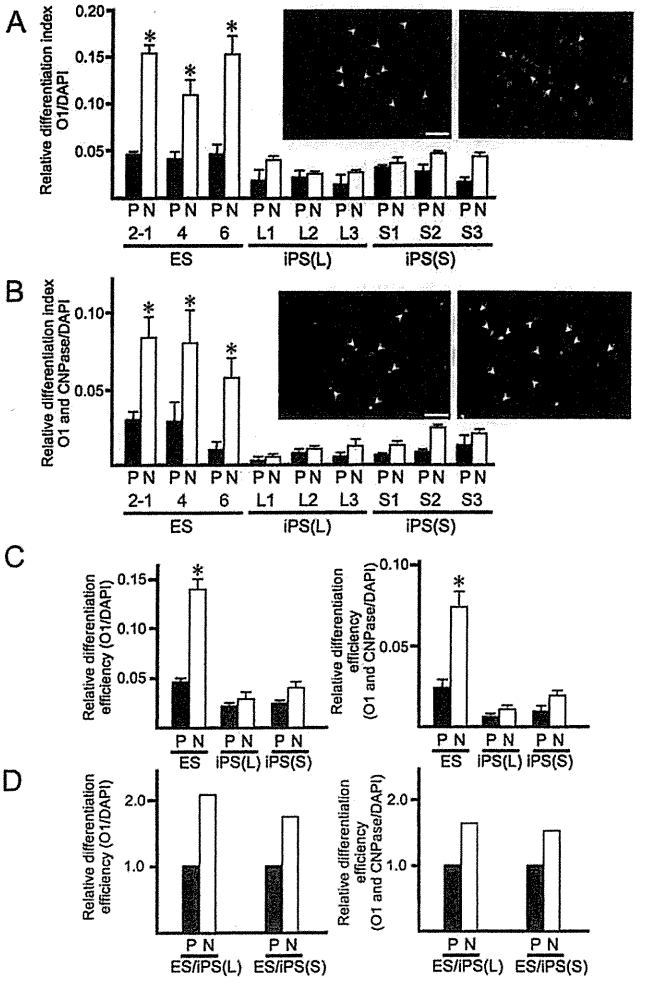

Fig. 2. Evaluation of the capacity for differentiation into oligodendrocytes among primed and naïve-like ESCs/iPSCs. Immunohistochemical detection of oligodendrocytes was evaluated using anti-O1 antibody (red) (A) and anti-O1 and anti-CNPase merged (orange) (B) signals (arrowheads) before (P) and after (N) naïve-like conversion of PSC lines. Mature oligodendrocytes with dendrites (arrows) were derived from naïve-like rdES2-1 cells (right panels). Quantification of the neural differentiation index of primed (P; closed bar) and naïve-like (N; open bar) rabbit ESC lines (rdES2-1, rdES4 and rdES6) and rabbit iPSC lines (liver-derived iPS-L1, iPS-L2 and iPS-L3 cells and stomach-derived iPS-S1, iPS-S2 and iPS-S3 cells). These signals were normalized to DAPI DNA staining signals. Data are shown as the mean ± SE (n = 3–7). *P < 0.05. Scale bar =100 μm. (C) Relative neural differentiation efficiencies of ESC lines and iPSC lines before (P; closed bar) and after (N; open bar) naïve-like conversion. Immunostaining signals for O1 (left graph) and O1/CNPase merged (right graph) from ESCs (rdES2-1, rdES4 and rdES6), liver-derived iPSCs (iPS-L1, iPS-L2 and iPS-L3) and stomach-derived iPSCs (iPS-S1, iPS-S2 and iPS-S3) have been averaged. Data are shown as the mean ± SE (n = 9–21). *P < 0.05. (D) The relative differentiation efficiencies before (P; closed bar) and after (N; open bar) naïve-like conversion of ESCs and iPSCs are shown. Immunostaining signals for O1 (left graph) and O1/CNPase merged (right graph) from ES cells (rdES2-1, rdES4 and rdES6) were normalized against liver-derived iPSCs (iPS-L1, iPS-L2 and iPS-L3) or stomach-derived iPSCs (iPS-S1, iPS-S2 and iPS-S3).

2B). Surprisingly, when naïve-like ESCs were examined, their *in vitro* differentiating capacity increased remarkably to 3.3–7.2 times that of naïve-like iPSCs (Fig. 2A–C). These results also suggested that the relative differentiation efficiencies of ESCs and iPSCs were enhanced by 1.5–2.1 times after naïve-like conversion (Fig. 2D). Interestingly, even though all ESC and iPSC lines were subjected to the same differentiating conditions, naïve-like converted rdES2-1 cells showed the best-developed ramified oligodendrocyte branches among all lines examined (Fig. 2A).

Chimeric rabbit production using naïve-like ESCs

Although naïve-like converted iPSCs have exhibited the capacity to be incorporated into the ICM of blastocysts, no chimeric contributions of these cells to more developed embryos or offspring have

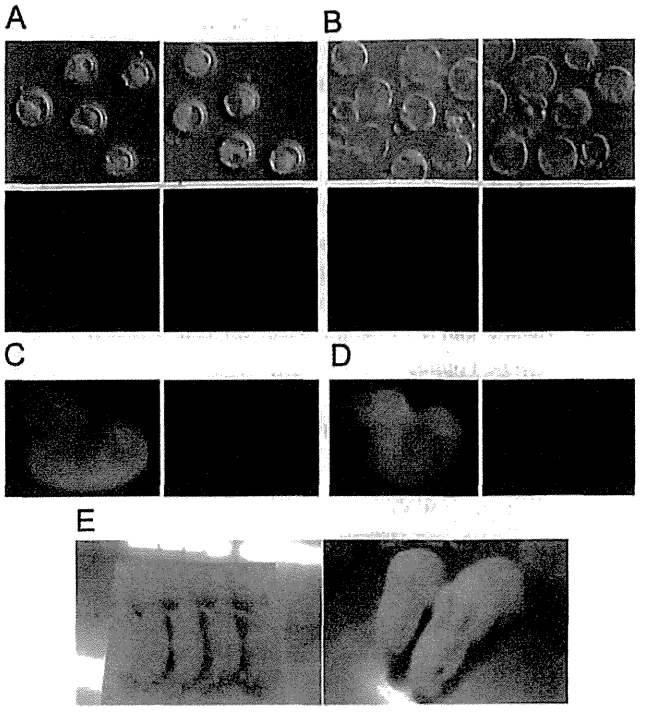

Fig. 3. Chimeric contribution of naïve-like ESCs in reconstructed embryos and pups. (A) EF1α–OCT3/4–GFP expression in rabbit blastocysts 48 h after an injection into 8-cell rabbit embryos of primed-state rdES2-1 cells (left panels) and naïve-like rdES2-1 cells (right panels). When primed-state ESCs were injected, putatively differentiated ESCs with almost no hOCT3/4–GFP expression did not contribute to the ICM of blastocysts. Scale bar = 100 μm. (B) EF1α–OCT3/4–GFP expression in interspecific (rabbit and mouse) blastocysts 48 h after injection into 8-cell mouse embryos of primed-state rdES2-1 cells (left panels) and naïve-like rdES2-1 cells (right panels). (C, D) Detection of chimeric contribution by GFP signals in a reconstructed rabbit embryo (15.5 dpc) (C) and interspecific (rabbit and mouse) embryo (11.5 dpc) (D). No GFP signal was observed (right panels). (E) Detection of chimeric contribution by black coat color. No chimeric contribution was observed in the pups (skin; left panel) or does (hair; right panel).

been examined [6]. Here we examined the chimeric contribution of naïve-like PSCs to developing embryos and pups using naïve-like ESCs with the highest capacity for *in vitro* differentiation (naïve-like rdES2-1 cells). As reported using rabbit iPSCs [6], naïve-like converted ESCs were injected into rabbit 8-cell embryos and cultured *in vitro* to allow the blastocysts to develop. As with the naïve-like iPSCs, the naïve-like ESCs readily colonized the ICMs of the blastocysts, maintaining homogeneous OCT3/4-GFP activity (Fig. 3A). Moreover, these naïve-like converted ESCs were readily incorporated into mouse blastocysts, forming interspecific chimeric rabbit/mouse embryos (Fig. 3B). Eight days after transplantation (11.5 dpc) into pseudopregnant female mice, embryos were recovered and examined for the presence of rabbit cells. However, no GFP signal was detected (Fig. 3D). The chimeric contributions of naïve-like rabbit ESCs to the developing rabbit embryos were assessed at 11 days after transplantation (15.5 dpc). Although these embryos developed normally, no GFP signal indicating a chimeric contribution was detected (Fig. 3C). Moreover, we could not obtain any evidence for chimeric contribution to these embryos even when using genomic PCR (data not shown). It is possible that the GFP signals indicating this could not be detected because of the disappearance of naïve-like ESCs at earlier stages of development *in vivo*. To convert naïve-like PSCs, we used lentivirus carrying the *OCT3/4* and *GFP* genes under the control of the *EF1α* promoter. Although this promoter is known to maintain the expression of transgenes in human ESCs [14], almost all of the GFP signals disappeared after the differentiation of rabbit iPSCs *in vitro* [6]. Because these naïve-like rdES2-1 cells had been established from Dutch belted rabbits (black skin and hair), we injected them into the embryos of Japanese White (JW) rabbits (white skin and hair) to detect any chimeric contribution. Of 105 injected embryos, 78 were transplanted into the oviducts of pseudopregnant JW rabbits. Ten of these (13%) developed to term. Six (8%) live pups were obtained (Table 1). To evaluate any possible chimeric contribution, the coat color (skin and hair) of the offspring was checked. However, none of the examined newborn pups (skin) or does (hair) had a black coat color (Fig. 3E).

Discussion

In this study, we generated naïve-like rabbit ESCs and assessed ability to differentiate *in vitro* into oligodendrocytes by comparing them with rabbit iPSCs. All of the PSC lines showed increased differentiation ability after naïve-like conversion. This highlights the differences in innate capacity among primed-state PSC lines. Although these pluripotent states can be termed "naïve-like" because of the difficulties in confirming a chimeric contribution in reconstructed offspring, our results provide a valuable strategy for the development of cell-based human regenerative medicine. We have already demonstrated that there is a relative differentiation potential of primed-state PSCs according to their origin in the following order: ESCs > stomach-derived iPSCs > liver-derived iPSCs; however, stomach-derived naïve-like iPSCs (not liver-derived naïve-like iPSCs) differentiated at an efficiency equivalent to or better than that of primed-state ESCs [6]. Here we found that naïve-like conversion of rabbit ESCs increased the differentiation capacity to a much greater level (3.3–7.2 times) than naïve-like converted iPSCs. Therefore, one of the most important points in this study is that the capacity for differentiation into oligodendrocytes of all PSCs increased after

Table 1. Development *in vivo* of embryos reconstructed using naïve-like rdES2-1 cells

Donor cells	Embryos injected	Embryos transferred	Pregnant/recipients	Retarded (% per ET)	Term conceptuses (% per ET)	Offspring (% per ET)
Naïve-like rdES2-1 cells	105	78	6/7	6 (7.7)	10 (12.8)	6 (7.7)

naïve-like conversion (Fig. 2A–C). This emphasizes the differences in innate capacity among primed-state PSC lines (Fig. 2D). Moreover, it was obvious that this relative differentiation order observed in primed-state PSCs was maintained even after naïve-like conversion.

There have been several studies on the differences in capacity of various forms of PSCs, and the patterns of global gene expression, DNA methylation and chromatin structures responsible for such variations have been analyzed carefully [15–18]. However, because of the variations between PSC lines, it is difficult to distinguish them from each other after extended culture [16]. Actually, rabbit iPSCs continued to be reprogrammed even after a number of passages, while becoming more similar to ESCs in their gene expression profiles [2]. Furthermore, repeated passages of these iPSCs permitted their differentiation into early neural cell types (neural stem cells, neurons and glial astrocytes) with efficiencies similar to ESCs [6]. Thus, *in vitro* differentiation systems seem to be effective for distinguishing differences between PSC lines [19–21]. Human iPSC lines derived from bone marrow cells, hair keratinocytes and skin fibroblasts were compared using *in vitro* differentiation into cardiomyocytes. All analyzed iPSCs could differentiate into cardiomyocytes, and the functional capacities of those derived from different cell origins were similar. However, bone marrow-derived iPSCs revealed a higher efficiency of cardiac differentiation than keratinocyte- and fibroblast-derived iPSCs [21]. On the other hand, the different potentials between ESCs and iPSCs could be overcome partly by modulating intracellular signaling pathways using chemical treatments, resulting in the efficient generation of desirable cell types, such as neural cells [22]. To understand donor cell specificity in iPSCs, it is very important to reveal the factors responsible for the differences in differentiating capacity between liver- and stomach-derived rabbit iPSCs. They need to be compared with ESCs established from liver cells and stomach cells using somatic cell nuclear transfer [23, 24].

Although the generation or conversion of naïve-like PSCs has been demonstrated using several animal species, the production of chimeric animals with a high contribution of donor cells and germline transmission has not yet been achieved [6, 25, 26]. We could not obtain any evidence of chimeric contribution in the embryos and offspring in this study, even when naïve-like rdES2-1 cells showing the best differentiating ability by *in vitro* assay were injected. These results indicated that we can now easily evaluate the quality of PSCs by neural differentiation following naïve-like conversion without the need to demonstrate chimeric contribution. We found here that the overexpression of *OCT3/4* and our culture environment were insufficient to produce true naïve (ground)-state PSCs. Although there have been several attempts to demonstrate that the overexpression of candidate genes (*KLF2* and *NANOG*) and/or that the treatment of primed-state PSCs with chemical inhibitors could produce naïve-state pluripotency [6, 10, 25, 27, 28], none of these studies confirmed this by chimeric contribution into the offspring or by germline transmission. Other techniques concerning the improved differentiation of mouse EpiSCs into ground-state PSCs have since been reported [29, 30]. These demonstrated the chimeric contribution and germline transmission of primed-state PSCs using modified culture conditions. Such indicators would confirm the derivation of true ground-state PSCs from nonrodent mammalian species. Using the rabbit, we can evaluate germline transmission easily. Although the derivation of true naïve PSCs could not be demonstrated in the present report, our system provides a powerful potential tool for deriving cells or tissues by *in vitro* differentiation using human iPS cells.

Acknowledgments

This work was supported by the Program to Disseminate Tenure Tracking System from the Ministry of Education, Culture, Sports, Science and Technology, PRESTO of the Japan Science and Technology Agency and a grant for basic science research projects from Sumitomo Foundation.

References

1. **Honda A, Hirose M, Inoue K, Ogonuki N, Miki H, Shimozawa N, Hatori M, Shimizu N, Murata T, Hirose M, Katayama K, Wakisaka N, Miyoshi H, Yokoyama KK, Sankai T, Ogura A.** Stable embryonic stem cell lines in rabbits: potential small animal models for human research. *Reprod Biomed Online* 2008; 17: 706–715.
2. **Honda A, Hirose M, Hatori M, Matoba S, Miyoshi H, Inoue K, Ogura A.** Generation of induced pluripotent stem cells in rabbits: potential experimental models for human regenerative medicine. *J Biol Chem* 2010; 285: 31362–31369.
3. **Graur D, Duret L, Gouy M.** Phylogenetic position of the order Lagomorpha (rabbits, hares and allies). *Nature* 1996; 379: 333–335.
4. **Shiomi M, Ito T, Yamada S, Kawashima S, Fan J.** Correlation of vulnerable coronary plaques to sudden cardiac events. Lessons from a myocardial infarction-prone animal model (the WHHLMI rabbit). *J Atheroscler Thromb* 2004; 11: 184–189.
5. **Weekers F, Van Herck E, Coopmans W, Michalaki M, Bowers CY, Veldhuis JD, Van den Berghe G.** A novel *in vivo* rabbit model of hypercatabolic critical illness reveals a biphasic neuroendocrine stress response. *Endocrinology* 2002; 143: 764–774.
6. **Honda A, Hatori M, Hirose M, Honda C, Izu H, Inoue K, Hirasawa R, Matoba S, Togayachi S, Miyoshi H, Ogura A.** Naive-like conversion overcomes the limited differentiation capacity of induced pluripotent stem cells. *J Biol Chem* 2013; 288: 26157–26166.
7. **Hanna J, Cheng AW, Saha K, Kim J, Lengner CJ, Soldner F, Cassady JP, Muffat J, Carey BW, Jaenisch R.** Human embryonic stem cells with biological and epigenetic characteristics similar to those of mouse ESCs. *Proc Natl Acad Sci USA* 2010; 107: 9222–9227.
8. **Rais Y, Zviran A, Geula S, Gafni O, Chomsky E, Viukov S, Mansour AA, Caspi I, Krupalnik V, Zerbib M, Maza I, Mor N, Baran D, Weinberger L, Jaitin DA, Lara-Astiaso D, Blecher-Gonen R, Shipony Z, Mukamel Z, Hagai T, Gilad S, Amann-Zalcenstein D, Tanay A, Amit I, Novershtern N, Hanna JH.** Deterministic direct reprogramming of somatic cells to pluripotency. *Nature* 2013; 502: 65–70.
9. **Ware CB, Nelson AM, Mecham B, Hesson J, Zhou W, Jonlin EC, Jimenez-Caliani AJ, Deng X, Cavanaugh C, Cook S, Tesar PJ, Okada J, Margaretha L, Sperber H, Choi M, Blau CA, Treuting PM, Hawkins RD, Cirulli V, Ruohola-Baker H.** Derivation of naive human embryonic stem cells. *Proc Natl Acad Sci USA* 2014; 111: 4484–4489.
10. **Theunissen TW, Powell BE, Wang H, Mitalipova M, Faddah DA, Reddy J, Fan ZP, Maetzel D, Ganz K, Shi L, Lungjangwa T, Imsoonthornruksa S, Stelzer Y, Rangarajan S, D'Alessio A, Zhang J, Gao Q, Dawlaty MM, Young RA, Gray NS, Jaenisch R.** Systematic identification of culture conditions for induction and maintenance of naive human pluripotency. *Cell Stem Cell* 2014; 15: 471–487.
11. **Nichols J, Smith A.** Naive and primed pluripotent states. *Cell Stem Cell* 2009; 4: 487–492.
12. **Brons IG, Smithers LE, Trotter MW, Rugg-Gunn P, Sun B, Chuva de Sousa Lopes SM, Howlett SK, Clarkson A, Ahrlund-Richter L, Pedersen RA, Vallier L.** Derivation of pluripotent epiblast stem cells from mammalian embryos. *Nature* 2007; 448: 191–195.
13. **Tesar PJ, Chenoweth JG, Brook FA, Davies TJ, Evans EP, Mack DL, Gardner RL, McKay RD.** New cell lines from mouse epiblast share defining features with human embryonic stem cells. *Nature* 2007; 448: 196–199.
14. **Kim S, Kim GJ, Miyoshi H, Moon SH, Ahn SE, Lee JH, Lee HJ, Cha KY, Chung HM.** Efficiency of the elongation factor-1alpha promoter in mammalian embryonic stem cells using lentiviral gene delivery systems. *Stem Cells Dev* 2007; 16: 537–545.
15. **Chin MH, Mason MJ, Xie W, Volinia S, Singer M, Peterson C, Ambartsumyan G, Aimiuwu O, Richter L, Zhang J, Khvorostov I, Ott V, Grunstein M, Lavon N, Benvenisty N, Croce CM, Clark AT, Baxter T, Pyle AD, Teitell MA, Pelegrini M, Plath K, Lowry WE.** Induced pluripotent stem cells and embryonic stem cells are distinguished by gene expression signatures. *Cell Stem Cell* 2009; 5: 111–123.
16. **Guenther MG, Frampton GM, Soldner F, Hockemeyer D, Mitalipova M, Jaenisch R,**

Young RA. Chromatin structure and gene expression programs of human embryonic and induced pluripotent stem cells. *Cell Stem Cell* 2010; 7: 249–257.

17. **Liang G, Zhang Y.** Genetic and epigenetic variations in iPSCs: potential causes and implications for application. *Cell Stem Cell* 2013; 13: 149–159.
18. **Mallon BS, Hamilton RS, Kozhich OA, Johnson KR, Fann YC, Rao MS, Robey PG.** Comparison of the molecular profiles of human embryonic and induced pluripotent stem cells of isogenic origin. *Stem Cell Res (Amst)* 2014; 12: 376–386.
19. **Kim K, Doi A, Wen B, Ng K, Zhao R, Cahan P, Kim J, Aryee MJ, Ji H, Ehrlich LI, Yabuuchi A, Takeuchi A, Cunniff KC, Hongguang H, McKinney-Freeman S, Naveiras O, Yoon TJ, Irizarry RA, Jung N, Seita J, Hanna J, Murakami P, Jaenisch R, Weissleder R, Orkin SH, Weissman IL, Feinberg AP, Daley GQ.** Epigenetic memory in induced pluripotent stem cells. *Nature* 2010; 467: 285–290.
20. **Osafune K, Caron L, Borowiak M, Martinez RJ, Fitz-Gerald CS, Sato Y, Cowan CA, Chien KR, Melton DA.** Marked differences in differentiation propensity among human embryonic stem cell lines. *Nat Biotechnol* 2008; 26: 313–315.
21. **Streckfuss-Bömeke K, Wolf F, Azizian A, Stauske M, Tiburcy M, Wagner S, Hübscher D, Dressel R, Chen S, Jende J, Wulf G, Lorenz V, Schön MP, Maier LS, Zimmermann WH, Hasenfuss G, Guan K.** Comparative study of human-induced pluripotent stem cells derived from bone marrow cells, hair keratinocytes, and skin fibroblasts. *Eur Heart J* 2013; 34: 2618–2629.
22. **Kim DS, Lee JS, Leem JW, Huh YJ, Kim JY, Kim HS, Park IH, Daley GQ, Hwang DY, Kim DW.** Robust enhancement of neural differentiation from human ES and iPS cells regardless of their innate difference in differentiation propensity. *Stem Cell Rev* 2010; 6: 270–281.
23. **Fang ZF, Gai H, Huang YZ, Li SG, Chen XJ, Shi JJ, Wu L, Liu A, Xu P, Sheng HZ.** Rabbit embryonic stem cell lines derived from fertilized, parthenogenetic or somatic cell nuclear transfer embryos. *Exp Cell Res* 2006; 312: 3669–3682.
24. **Zakhartchenko V, Flisikowska T, Li S, Richter T, Wieland H, Durkovic M, Rottmann O, Kessler B, Gungor T, Brem G, Kind A, Wolf E, Schnieke A.** Cell-mediated transgenesis in rabbits: chimeric and nuclear transfer animals. *Biol Reprod* 2011; 84: 229–237.
25. **Fujishiro SH, Nakano K, Mizukami Y, Azami T, Arai Y, Matsunari H, Ishino R, Nishimura T, Watanabe M, Abe T, Furukawa Y, Umeyama K, Yamanaka S, Ema M, Nagashima H, Hanazono Y.** Generation of naive-like porcine-induced pluripotent stem cells capable of contributing to embryonic and fetal development. *Stem Cells Dev* 2013; 22: 473–482.
26. **Osteil P, Tapponnier Y, Markossian S, Godet M, Schmaltz-Panneau B, Jouneau L, Cabau C, Joly T, Blachère T, Gócza E, Bernat A, Yerle M, Acloque H, Hidot S, Bosze Z, Duranthon V, Savatier P, Afanassieff M.** Induced pluripotent stem cells derived from rabbits exhibit some characteristics of naïve pluripotency. *Biol Open* 2013; 2: 613–628.
27. **Gafni O, Weinberger L, Mansour AA, Manor YS, Chomsky E, Ben-Yosef D, Kalma Y, Viukov S, Maza I, Zviran A, Rais Y, Shipony Z, Mukamel Z, Krupalnik V, Zerbib M, Geula S, Caspi I, Schneir D, Shwartz T, Gilad S, Amann-Zalcenstein D, Benjamin S, Amit I, Tanay A, Massarwa R, Novershtern N, Hanna JH.** Derivation of novel human ground state naive pluripotent stem cells. *Nature* 2013; 504: 282–286.
28. **Takashima Y, Guo Ge, Loos, R, Nichols J, Ficz G, Krueger F, Oxley D, Santos F, Clarke J, Mansfield W, Reik W, Bertone P, Smith A.** Resetting transcription factor control circuitry toward ground-state pluripotency in human. *Cell Stem Cell.*, in press.
29. **Sumi T, Oki S, Kitajima K, Meno C.** Epiblast ground state is controlled by canonical Wnt/β-catenin signaling in the postimplantation mouse embryo and epiblast stem cells. *PLoS ONE* 2013; 8: e63378.
30. **Tsukiyama T, Ohinata Y.** A modified EpiSC culture condition containing a GSK3 inhibitor can support germline-competent pluripotency in mice. *PLoS ONE* 2014; 9: e95329.

Exp. Anim. 64(1), 31–37, 2015

—Original—

Single-step generation of rabbits carrying a targeted allele of the tyrosinase gene using CRISPR/Cas9

Arata HONDA[1, 2)*], Michiko HIROSE[2)*], Tadashi SANKAI[3)], Lubna YASMIN[3)], Kazuaki YUZAWA[3)], Kimiko HONSHO[1)], Haruna IZU[1)], Atsushi IGUCHI[4)], Masahito IKAWA[5)], and Atsuo OGURA[2)]

[1)] *Organization for Promotion of Tenure Track, University of Miyazaki, 5200, Kibara, Kiyotake, Miyazaki 889-1692, Japan*
[2)] *RIKEN BioResource Center, Tsukuba, Ibaraki 305-0074, Japan*
[3)] *Tsukuba Primate Research Center, National Institute of Biomedical Innovation, Tsukuba, Ibaraki 305-0843, Japan*
[4)] *Interdisciplinary Research Organization, University of Miyazaki, Miyazaki 889-1692, Japan*
[5)] *Research Institute for Microbial Diseases, Osaka University, Suita, Osaka 556-0871, Japan*

Abstract: Targeted genome editing of nonrodent mammalian species has provided the potential for highly accurate interventions into gene function in humans and the generation of useful animal models of human diseases. Here we show successful clustered regularly interspaced short palindromic repeat (CRISPR) and CRISPR-associated (Cas)-mediated gene targeting via circular plasmid injection in rabbits. The rabbit tyrosinase gene (*TYR*) was effectively disrupted, and we confirmed germline transmission by pronuclear injection of a circular plasmid expressing humanized Cas9 (hCas9) and single-guide RNA. Direct injection into pronuclear stage zygotes was possible following an *in vitro* validation assay. Neither off-target mutagenesis nor hCas9 transgenesis was detected in any of the genetically targeted pups and embryos examined. Gene targeting with this rapid and simplified strategy will help accelerate the development of translational research using other nonrodent mammalian species.

Key words: CRISPR/Cas9, gene targeting, rabbit, tyrosinase

Introduction

Gene targeting and disruption in mice are valuable tools for understanding gene function in mammalian development and disease [2]. They generally involve the production of chimeric progeny using homologous recombined pluripotent stem cells (PSCs), which have the ability to transmit their genome into the germline (naïve PSCs). However, effective germline transmission of PSCs in chimeric animals has so far been achieved only in the mouse and rat (rodent species) [15]. Pluripotent stem cells in nonrodent mammalian species have been generated as primed-state PSCs, but these have proved difficult to include in the embryo proper when introduced into host preimplantation embryos [8, 20].

Recently engineered endonucleases, such as zinc-finger nucleases (ZFNs) and transcription activator-like effector nucleases (TALENs), are useful for gene targeting [7]. They allow efficient and specific cleavage of genomic sequences in animals by directly injecting mRNAs of site-specific nucleases into 1-cell embryos to generate a double-strand breakage (DSB) in the DNA

(Received 8 April 2014 / Accepted 18 July 2014 / Published online in J-STAGE 8 September 2014)
Address corresponding: A. Honda, Organization for Promotion of Tenure Track, University of Miyazaki, 5200, Kibara, Kiyotake, Miyazaki 889-1692, Japan
Supplementary tables and figure: refer to J-STAGE: https://www.jstage.jst.go.jp/browse/expanim
**These authors contributed equally to this work.*

[7]. The enzymes recognize target DNA by peptide-DNA affinity, and fused FokI nucleases generate a DSB; subsequently, error-prone nonhomologous end joining results in small insertions or deletions (indels). However, even though several methods such as Golden Gate assembly [4] or the Platinum Gate system [18] have been developed to decrease the steps, the complex and time-consuming design and generation of ZFNs or TALENs for each target gene limit the application of these methods.

The type II bacterial clustered regularly interspaced short palindromic repeat (CRISPR) and CRISPR-associated protein (Cas) have been developed as an efficient gene targeting system [10]. In such type II systems, the complex of a CRISPR RNA (crRNA) annealed to a trans-activating crRNA is sufficient to guide the Cas9 endonuclease to a specific genomic sequence to generate a DSB in the target DNA. Recent reports demonstrated gene targeting of several genes in mice and rats using the CRISPR/Cas system [11, 21]. The ease of design, construction, and delivery of multiple synthetic single-guide RNAs (sgRNAs) suggest the possibility of multiplexed genome editing in mammals [21]. Recent studies of Cas9 specificity have demonstrated that although each base within the 20 nt guide sequence contributes to its overall specificity, multiple mismatches between the sgRNA and its complementary target DNA sequence can be tolerated depending on the quantity, position, and base identity of the mismatches [11].

This leads to potential off-target DSBs and indel formation [6, 9]. To improve the specificity of Cas9-mediated genome editing, a combination of the D10A mutant nickase version of Cas9 with a pair of offset sgRNAs complementary to opposite strands of the target site has been suggested [17]. Generally, for targeted disruption of a candidate gene in mammalian embryos, the injected mRNA must be prepared using several steps. Target sequences need to be evaluated by *in vitro* assay using plasmid vectors, reconstruction of mRNA expression vectors, and then preparation of the desired mRNA by *in vitro* transcription [12, 17, 20, 22, 23, 24]. However, Mashiko *et al.* reported direct injection of a plasmid DNA, pX330 [5], containing a humanized Cas9 (hCas9) expression cassette with a gene-targeting sgRNA expression cassette. This enabled a rapid (within 1 month), simple, and reproducible method for targeted mutagenesis in mice [13]. For these reasons, the CRISPR/Cas9 system is now developing as a valuable strategy for genome editing research and possibly for generating targeted gene modification in nonrodent mammalian species [16, 23].

Here we confirmed successful gene targeting in the rabbit via a simplified and rapid strategy using pX330, a circular plasmid DNA encoding hCas9, and sgRNA. Thus, we demonstrated efficient generation of a genetically engineered nonrodent mammalian species. Potentially, this approach could be used for the functional annotation of genes or for modeling human genetic diseases.

Materials and Methods

Animals

All rabbits were maintained and used for experiments in accordance with the guidelines for animal experimentation of the RIKEN Bioresource Center and Tsukuba Primate Research Center after approval by the responsible committees.

Plasmid preparation

To perform the single-strand annealing (SSA) assay, a pCAG-EGxxFP plasmid expressing a 5′ and 3′ enhanced green fluorescent protein (EGFP) sequence was used according to Mashiko *et al.* [13]. The 499-bp genomic fragment of the rabbit tyrosinase gene containing an sgRNA target sequence was amplified by polymerase chain reaction (PCR) with a cycling program of 94°C for 3 min and 35 cycles of 94°C for 30 s, 60°C for 30 s, and 72°C for 30 s and placed between the EGFP fragments at the multiple cloning site (*Bam*HI–*Eco*RI) of pCAG-EGxxFP. Plasmids coexpressing hCas9 and sgRNA were prepared by ligating oligonucleotides into the *Bbs*I site of pX330 (http://www.addgene.org/42230/). The primers and oligonucleotides used are listed in Table S1.

Cell transfection

Ten micrograms of pCAG-EGxxFP-target was mixed with 10 μg of pX330 with or without the sgRNA sequence and then introduced with a NEPA21 electroporator (Nepa Gene Co., Ltd., Chiba, Japan) into 3×10^5 human embryonic kidney (HEK) 293 cells/well cultured in 6-well plates. The EGFP fluorescence was observed and assessed using a fluorescence microscope (model BZ-9000; Keyence, Osaka, Japan) and a BZ-II Analyzer image analysis system (Keyence).

Production of the rabbits carrying the targeted allele of the tyrosinase gene

Mature Dutch Belted rabbits were purchased from Kitayama Labes (Nagano, Japan). Fertilized embryos were obtained from mature female rabbits that had been treated with 75 IU of follicle stimulating hormone (Antrin R10; Kyoritsu Seiyaku, Tokyo, Japan) twice daily for 3 days, followed by 100 IU of human chorionic gonadotropin (hCG; Gonatropin; Teikoku Zoki, Tokyo, Japan) 12 h later. The does were mated with fertile males immediately after hCG treatment. Twenty hours after mating, fertilized embryos (zygotes) were flushed from the oviducts using warmed HEPES-buffered RD medium [3] containing 4 mg/ml of bovine serum albumin (ICN Biomedicals, Irvine, CA, USA). The pronuclei of zygotes were microinjected with 5 ng/μl of the pX330 plasmid. After pronuclear injection of the plasmid, the embryos were cultured in RD medium at 37°C in 6% CO_2 and 5% O_2 in air for 24 h and then transferred into the oviducts of pseudopregnant Japanese White (JW) rabbits (Kitayama Labes) that had been treated with 100 IU hCG and given manual vulval stimulation 24 h before transfer. To confirm germline transmission, a heterozygous mutant female rabbit that had a targeted allele of the tyrosinase gene, was mated with male JW rabbit. For genotyping of the offspring, skin samples were collected 2-days after birth, and genomic DNAs were extracted and sequenced.

DNA sequencing

Genomic DNA was extracted from small tissues of embryos or pups. Approximately 500–700 bp genomic fragments containing the target site were amplified by PCR and sequenced. After confirmation of an indel mutation at the target site, PCR fragments were subcloned into a pT7 Blue T-vector (Merck Millipore, Darmstadt, Germany) and sequenced for the determination of each allele.

Off-target analysis

According to Yang *et al.*, each sgRNA of the 12 nt target sequence immediately upstream of the Protospacer Adjacent Motif (PAM) and the 3 nt PAM sequence (NGG, with four variations, i.e., AGG, TGG, GGG, CGG) was searched against the rabbit genome in Ensembl (http://www.ensembl.org/Oryctolagus_cuniculus/Info/Index). The "E value" was set to 100000. The number of exactly matched sequences in the query results was the total number of hits in the rabbit genome, including the designed target sequence. If the hit was within an exon region (defined as from 100 bp upstream to 100 bp downstream of any exon based on the Ensembl output), we considered it as a significant hit and considered a potential off target site. PCR and sequencing were conducted on potential off-target loci to identify if there were any mutations. Moreover, the other potential off-target sites were analyzed using BLAST searching of the *Oryctolagus cuniculus*(rabbit) nucleotide sequences (http://www.ncbi.nlm.nih.gov/BLAST/). Twenty bases preceding the PAM sequence were aligned with the rabbit genome. Approximately 500–700 bp genomic fragments containing a centrally situated off-target site were amplified by PCR and sequenced. The primers used for off-target PCR analysis are listed in Table S1.

Results

Evaluation of sgRNA Sequences to disrupt the rabbit Tyrosinase Gene Using CRISPR/Cas9

To establish a system that could produce genetically targeted rabbits effectively, we used the pX330 plasmid expressing hCas9 and sgRNA for serial gene targeting, after assessing the efficacy of producing appropriate DSBs by SSA assays *in vitro* [13]. The efficacy of DSB-mediated homology-dependent repair was validated by cotransfection with the plasmid pCAG-EGxxFP (Fig. 1A). This system does not need to construct additional plasmids or require the use of further sgRNA synthesis for the microinjection of CRISPR/Cas9 after evaluating nuclease activity. To disrupt the rabbit tyrosinase gene, four target sites in the first exon were evaluated by SSA assays (Fig. 1B). Each pX330 plasmid was co-transfected with pCAG-EGxxFP, which contains a 499-bp genomic fragment of tyrosinase containing sgRNA target sequences. EGFP fluorescence was evaluated to determine which sgRNA sequence in pX330 caused a DSB in the pCAG-EGxxFP sequence in HEK293T cells (Figs. 2A and B). A candidate sequence, tyrosinase CR2, showed the most effectiveness in causing a suitable DSB.

Single-step production of genetically targeted rabbits using CRISPR/Cas9

Following validation of the sgRNA sequence by SSA assay, the most effective plasmid—pX330 with the target sequence tyrosinase CR2—was microinjected directly into the pronuclei of rabbit zygotes. Of 77 injected eggs,

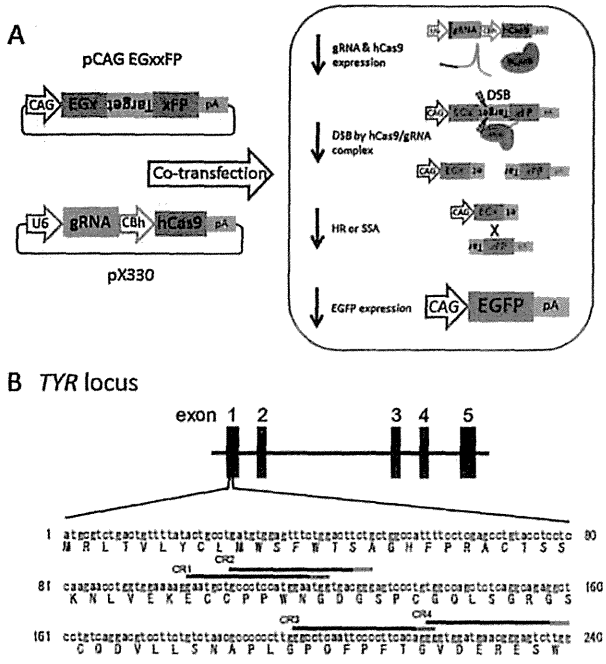

Fig. 1. Scheme for CRISPR/Cas9-mediated gene targeting. (A) Scheme for the SSA assay using pCAG EGxxFP and pX330 in HEK293 cells. The transduced hCas9 and sgRNA complex caused DSB in the target sequence of pCAG-EGxxFP by homology-dependent repair via homologous recombination (HR) or caused single-strand annealing (SSA). (B) Schematic representation of sgRNAs targeting tyrosinase (*TYR*). The sgRNA target sequence and PAM sequence are highlighted in black and red, respectively.

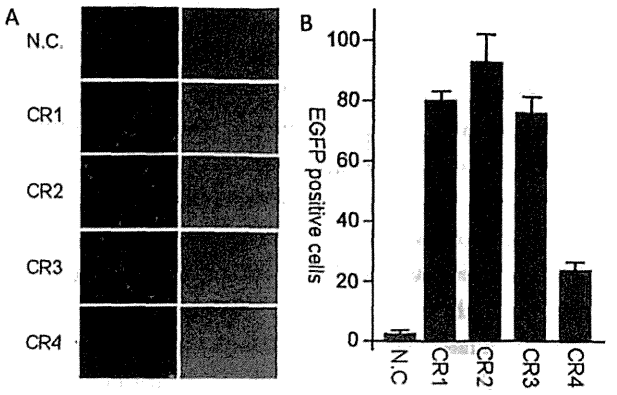

Fig. 2. Evaluation of sgRNA sequences for disrupting the rabbit tyrosinase gene. (A) The efficiency of DSB-mediated homology-dependent repair was validated by observing EGFP fluorescence at 24 h after transfection (left panels, EGFP signals; right panels, phase contrast microscopy images). (N.C., normal control pX330 without an sgRNA sequence; CR1-CR4, pX330 plasmid with tyrosinase CR1/CR2/CR3/CR4 sequences, respectively). (B) Quantitative representation of the DSB efficiency of each sgRNA sequence. Data are shown as the mean ± standard deviation (SD). Scale bar=100 μm.

Table 1. Generation of genetically targeted rabbits using CRISPR/Cas9

	Injected	Survived	Pups	GMO (hetero:homo)
Tyrosinase CR2	77	67 (87%)	9 (13%)	2 (3%) (1:1)

GMO, genetically modified organism.

67 (87%) embryos were transplanted into the oviducts of pseudopregnant JW rabbits. Nine of these (13%) developed to term. Of them, two (3%) pups had the targeted allele at the tyrosinase locus (Table 1). One live pup with a normal coat color (Dutch Belted) had a heterozygous mutation (a 2-bp deletion) at the tyrosinase locus (Fig. 3A). Unfortunately, one pup with an albino coat-color phenotype over its entire body that carried a homozygous mutation (a 7-bp deletion) at the tyrosinase locus was stillborn (Fig. S1). Two of the wild-type pups also died prenatally. To detect off-target mutations in mutant pups, 20-base sequences of the sgRNA sequence of tyrosinase CR2 were searched in the rabbit genome using Ensemble and BLAST. Five potential off-target sites with two or three mismatch sequences were found (Supplementary Table S2). We amplified and sequenced the genomic DNAs around the regions that contained the potential off-target sites in these mutant rabbits. No off-target mutations were detected. Additionally, no hCas9 transgenes were detected in any of the pups examined (data not shown). To confirm germline transmission, a heterozygous female mutant rabbit that showed a Dutch coat color was crossed with a male JW rabbit. We successfully obtained does that had the white coat color phenotype over their entire body and red eyes (Fig. 3B and C). In fact, sequencing analysis suggested that the white does carried the targeted allels of the tyrosinase gene (Fig. 3B). Thus, pronuclear injection of this circular plasmid DNA proved to be a very effective strategy for the generation of genetically targeted rabbits using CRISPR/Cas9.

Discussion

In this report, we document simplified gene targeting via the CRISPR/Cas9 system in the rabbit. Using microinjection of pronuclei with our circular plasmid DNA—validated by *in vitro* SSA—it was not necessary to reconstruct mRNA expression vectors, to carry out sequence confirmation, or to prepare mRNAs by *in vitro* transcription as reported previously [12, 17, 20, 22, 23,

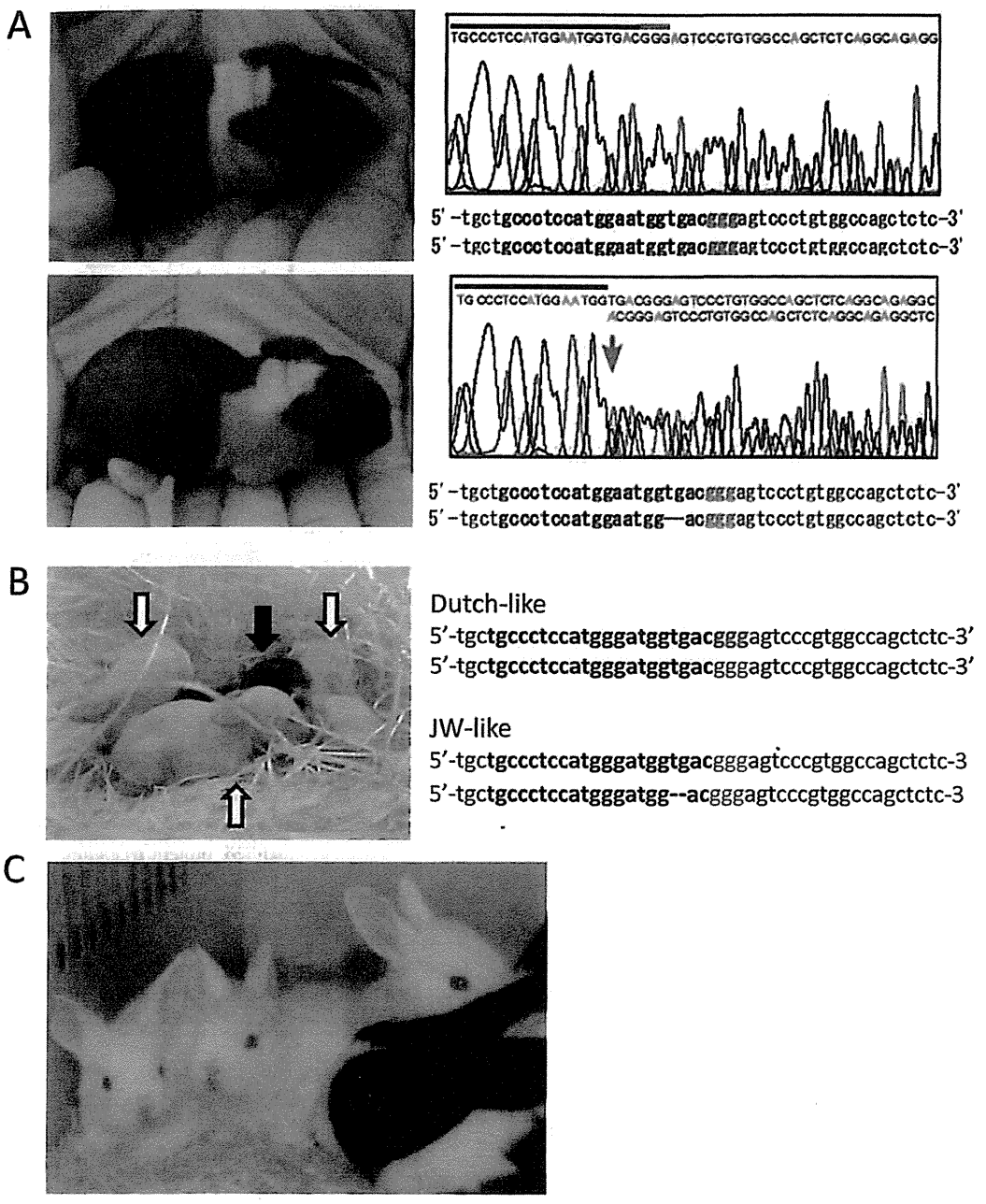

Fig. 3. CRISPR/Cas9-mediated modification of the tyrosinase gene in founder rabbits. (A) Five-day-old founder pups with representative tyrosinase genomic sequences (top panels, wild-type pup; bottom panels, heterozygous pup with a 2-bp deletion). The arrow indicates the indel mutation in this pup. Subcloning and sequencing its PCR fragment confirmed each allele's identity. (B) Photograph and representative tyrosinase genomic sequences of F1 pups that showed a Dutch-like coat color (closed arrow) and JW-like (white) coat color (open arrows). (C) Photograph of JW-like does that have a white coat color and red eyes.

24]. Because no off-target mutation or hCas9 transgenesis was detected in this experiment, this method of circular plasmid DNA injection into zygotes will be a valuable and rapid strategy for achieving gene targeting not only in rodents but also in other mammalian species.

In the mouse model, gene knockout and knockin via cytoplasmic coinjection of mRNAs encoding hCas9 and sgRNA have been used widely and successfully [17, 20, 24]. Mashiko *et al.* [13] have reported that the pronuclear injection of a circular plasmid expressing the hCas9/

sgRNA complex is a rapid, simple, and reproducible method for achieving targeted mutagenesis in mice. This method can skip the need for constructing mRNA expression vectors and sgRNA synthesis. Here we employed this strategy in the rabbit and showed its easy and rapid capacity to accomplish gene targeting with high accuracy. Although no transgene was detected in our experiments, fewer than 5% of the genetically targeted offspring expressed the hCas9 transgene in the mouse system [12]. Moreover, compared with mouse data in general (more than 10% of genetically modified offspring per injected embryos), the success rate of our experiment (3%) seems low. It is well known that the efficiency of gene transfer into rabbits by the microinjection of plasmid-based constructs into pronuclei varies between 0.5% and 3% [1]. Rabbit pronuclear-stage embryos seem to have much more chromosomal fragility than mouse embryos. Therefore, we need to assess the efficiency of gene modification in the rabbit using plasmid microinjection not into the pronuclei but also into the zygote cytoplasm to prevent hCas9 transgenesis and/or to prevent chromosomal damage. Unfortunately, one albino pup carrying a homozygous mutation (a 7-bp deletion) at the tyrosinase locus was stillborn (Fig. 3). A null mutation in tyrosinase was unlikely to be the cause of this death, as two wild-type pups also died prenatally in this experiment and healthy offspring carrying tyrosinase null mutations have been born in other laboratories [14, 19]. Some unidentified genetic aberrations might have occurred during micromanipulation of the oocytes and embryos. We successfully confirmed germline transmission of the targeted allele and the effect in the form of the white coat color phenotype by natural mating using the heterozygous mutant individual with a JW rabbit.

This report offers a valuable candidate strategy for appropriate gene targeting using the CRISPR/Cas9 system in the rabbit. This will facilitate investigations of gene function and the production of useful animal models of human diseases.

Abbreviations

Cas, CRISPR-associated; hCas9, humanized Cas9; CRISPR, clustered regularly interspaced short palindromic repeat; crRNA, CRISPR RNA; DSB, double-strand break; EGFP, enhanced green fluorescence protein; FSH, follicle stimulating hormone; GMO, genetically modified organism; hCG, human chorionic gonadotropin; JW, Japanese White; NHEJ, nonhomologous end joining; PAM, Protospacer Adjacent Motif; PCR, polymerase chain reaction; PSC, pluripotent stem cell; sgRNA, single-guide RNA; SSA, single-strand annealing; TALEN, transcription activator-like effector nuclease; ZFN, zinc-finger nuclease.

Acknowledgments

This work was supported by the Program to Disseminate the Tenure Tracking System from of the Ministry of Education, Culture, Sports, Science and Technology of Japan and the PRESTO program of the Japan Science and Technology Agency.

References

1. Bosze, Z., Hiripi, L., Carnwath, J.W., and Niemann, H. 2003. The transgenic rabbit as model for human diseases and as a source of biologically active recombinant proteins. *Transgenic. Res.* 12: 541–553. [Medline] [CrossRef]
2. Capecchi, M.R. 2005. Gene targeting in mice: functional analysis of the mammalian genome for the twenty-first century. *Nat. Rev. Genet.* 6: 507–512. [Medline] [CrossRef]
3. Carney, E.W. and Foote, R.H. 1991. Improved development of rabbit one-cell embryos to the hatching blastocyst stage by culture in a defined, protein-free culture medium. *J. Reprod. Fertil.* 91: 113–123. [Medline] [CrossRef]
4. Cermak, T., Doyle, E.L., Christian, M., Wang, L., Zhang, Y., Schmidt, C., Baller, J.A., Somia, N.V., Bogdanove, A.J., and Voytas, D.F. 2011. Efficient design and assembly of custom TALEN and other TAL effector-based constructs for DNA targeting. *Nucleic. Acids. Res.* 39: e82. [Medline] [CrossRef]
5. Cong, L., Ran, F.A., Cox, D., Lin, S., Barretto, R., Habib, N., Hsu, P.D., Wu, X., Jiang, W., Marraffini, L.A., and Zhang, F. 2013. Multiplex genome engineering using CRISPR/Cas systems. *Science* 339: 819–823. [Medline] [CrossRef]
6. Fu, Y., Foden, J.A., Khayter, C., Maeder, M.L., Reyon, D., Joung, J.K., and Sander, J.D. 2013. High-frequency off-target mutagenesis induced by CRISPR-Cas nucleases in human cells. *Nat. Biotechnol.* 31: 822–826. [Medline] [CrossRef]
7. Gaj, T., Gersbach, C.A., and Barbas, C.F. 3rd. 2013. ZFN, TALEN, and CRISPR/Cas-based methods for genome engineering. *Trends Biotechnol.* 31: 397–405. [Medline] [CrossRef]
8. Honda, A., Hatori, M., Hirose, M., Honda, C., Izu, H., Inoue, K., Hirasawa, R., Matoba, S., Togayachi, S., Miyoshi, H., and Ogura, A. 2013. Naive-like conversion overcomes the limited differentiation capacity of induced pluripotent stem cells. *J. Biol. Chem.* 288: 26157–26166. [Medline] [CrossRef]

9. Hsu, P.D., Scott, D.A., Weinstein, J.A., Ran, F.A., Konermann, S., Agarwala, V., Li, Y., Fine, E.J., Wu, X., Shalem, O., Cradick, T.J., Marraffini, L.A., Bao, G., and Zhang, F. 2013. DNA targeting specificity of RNA-guided Cas9 nucleases. *Nat. Biotechnol.* 31: 827–832. [Medline] [CrossRef]
10. Jinek, M., Chylinski, K., Fonfara, I., Hauer, M., Doudna, J.A., and Charpentier, E. 2012. A programmable dual-RNA-guided DNA endonuclease in adaptive bacterial immunity. *Science* 337: 816–821. [Medline] [CrossRef]
11. Kuscu, C., Arslan, S., Singh, R., Thorpe, J., and Adli, M. 2014. Genome-wide analysis reveals characteristics of off-target sites bound by the Cas9 endonuclease. *Nat. Biotechnol.* 32: 677–683. [Medline] [CrossRef]
12. Li, D., Qiu, Z., Shao, Y., Chen, Y., Guan, Y., Liu, M., Li, Y., Gao, N., Wang, L., Lu, X., Zhao, Y., and Liu, M. 2013. Heritable gene targeting in the mouse and rat using a CRISPR-Cas system. *Nat. Biotechnol.* 31: 681–683. [Medline] [CrossRef]
13. Mashiko, D., Fujihara, Y., Satouh, Y., Miyata, H., Isotani, A., and Ikawa, M. 2013. Generation of mutant mice by pronuclear injection of circular plasmid expressing Cas9 and single guided RNA. *Sci. Rep.* 3: 3355. [Medline] [CrossRef]
14. Mashimo, T., Kaneko, T., Sakuma, T., Kobayashi, J., Kunihiro, Y., Voigt, B., Yamamoto, T., and Serikawa, T. 2013. Efficient gene targeting by TAL effector nucleases coinjected with exonucleases in zygotes. *Sci. Rep.* 3: 1253. [Medline] [CrossRef]
15. Nichols, J. and Smith, A. 2009. Naive and primed pluripotent states. *Cell Stem Cell* 4: 487–492. [Medline] [CrossRef]
16. Niu, Y., Shen, B., Cui, Y., Chen, Y., Wang, J., Wang, L., Kang, Y., Zhao, X., Si, W., Li, W., Xiang, A.P., Zhou, J., Guo, X., Bi, Y., Si, C., Hu, B., Dong, G., Wang, H., Zhou, Z., Li, T., Tan, T., Pu, X., Wang, F., Ji, S., Zhou, Q., Huang, X., Ji, W., and Sha, J. 2014. Generation of gene-modified cynomolgus monkey via Cas9/RNA-mediated gene targeting in one-cell embryos. *Cell* 156: 836–843. [Medline] [CrossRef]
17. Ran, F.A., Hsu, P.D., Lin, C.Y., Gootenberg, J.S., Konermann, S., Trevino, A.E., Scott, D.A., Inoue, A., Matoba, S., Zhang, Y., and Zhang, F. 2013. Double nicking by RNA-guided CRISPR Cas9 for enhanced genome editing specificity. *Cell* 154: 1380–1389. [Medline] [CrossRef]
18. Sakuma, T., Ochiai, H., Kaneko, T., Mashimo, T., Tokumasu, D., Sakane, Y., Suzuki, K., Miyamoto, T., Sakamoto, N., Matsuura, S., and Yamamoto, T. 2013. Repeating pattern of non-RVD variations in DNA-binding modules enhances TALEN activity. *Sci. Rep.* 3: 3379. [Medline] [CrossRef]
19. Suzuki, K.T., Isoyama, Y., Kashiwagi, K., Sakuma, T., Ochiai, H., Sakamoto, N., Furuno, N., Kashiwagi, A., and Yamamoto, T. 2013. High efficiency TALENs enable F0 functional analysis by targeted gene disruption in Xenopus laevis embryos. *Biol. Open* 2: 448–452. [Medline] [CrossRef]
20. Tachibana, M., Sparman, M., Ramsey, C., Ma, H., Lee, H.S., Penedo, M.C., and Mitalipov, S. 2012. Generation of chimeric rhesus monkeys. *Cell* 148: 285–295. [Medline] [CrossRef]
21. Wang, H., Yang, H., Shivalila, C.S., Dawlaty, M.M., Cheng, A.W., Zhang, F., and Jaenisch, R. 2013. One-step generation of mice carrying mutations in multiple genes by CRISPR/Cas-mediated genome engineering. *Cell* 153: 910–918. [Medline] [CrossRef]
22. Xiao, A., Wang, Z., Hu, Y., Wu, Y., Luo, Z., Yang, Z., Zu, Y., Li, W., Huang, P., Tong, X., Zhu, Z., Lin, S., and Zhang, B. 2013. Chromosomal deletions and inversions mediated by TALENs and CRISPR/Cas in zebrafish. *Nucleic Acids Res.* 41: e141. [Medline] [CrossRef]
23. Yang, D., Xu, J., Zhu, T., Fan, J., Lai, L., Zhang, J., and Chen, Y.E. 2014. Effective gene targeting in rabbits using RNA-guided Cas9 nucleases. *J. Mol. Cell Biol.* 6: 97–99. [Medline] [CrossRef]
24. Yang, H., Wang, H., Shivalila, C.S., Cheng, A.W., Shi, L., and Jaenisch, R. 2013. One-step generation of mice carrying reporter and conditional alleles by CRISPR/Cas-mediated genome engineering. *Cell* 154: 1370–1379. [Medline] [CrossRef]

Comparative Medicine
Copyright 2014
by the American Association for Laboratory Animal Science

Vol 64, No 2
April 2014
Pages 140–147

Original Research

Role of Retinoic Acid and Fibroblast Growth Factor 2 in Neural Differentiation from Cynomolgus Monkey (*Macaca fascicularis*) Embryonic Stem Cells

Masanori Hatori,[1,2] Nobuhiro Shimozawa,[1] Lubna Yasmin,[1] Hirofumi Suemori,[3] Norio Nakatsuji,[3,4] Atsuo Ogura,[5,6] Ken-ichi Yagami,[2] and Tadashi Sankai[1,*]

Retinoic acid is a widely used factor in both mouse and human embryonic stem cells. It suppresses differentiation to mesoderm and enhances differentiation to ectoderm. Fibroblast growth factor 2 (FGF2) is widely used to induce differentiation to neurons in mice, yet in primates, including humans, it maintains embryonic stem cells in the undifferentiated state. In this study, we established an FGF2 low-dose-dependent embryonic stem cell line from cynomolgus monkeys and then analyzed neural differentiation in cultures supplemented with retinoic acid and FGF2. When only retinoic acid was added to culture, neurons differentiated from FGF2 low-dose-dependent embryonic stem cells. When both retinoic acid and FGF2 were added, neurons and astrocytes differentiated from the same embryonic stem cell line. Thus, retinoic acid promotes the differentiation from embryonic stem cells to neuroectoderm. Although FGF2 seems to promote self-renewal in stem cells, its effects on the differentiation of stem cells are influenced by the presence or absence of supplemental retinoic acid.

Abbreviations: EB, embryoid body; ES, embryonic stem; ESM, embryonic stem cell medium; FGF, fibroblast growth factor; GFAP, glial fibrillary acidic protein; LIF, leukemia inhibitory factor; MBP, myelin basic protein; RA, retinoic acid; SSEA, stage-specific embryonic antigen; TRA, tumor-related antigen.

Pluripotent stem cells are potential sources of material for cell replacement therapy and are useful experimental tools for in vitro models of human disease and drug screening. Embryonic stem (ES) cells are capable of extensive proliferation and multilineage differentiation, and thus ES-derived cells are suitable for use in cell-replacement therapies.[18,23] Reported ES cell characteristics including tumorigenic potential, DNA methylation status, expression of imprinted genes, and chromatin structure were elucidated by using induced pluripotent stem cells.[2,11,17] Because the social expectations of regeneration medicine are growing, we must perform basic research with ES cells, which differ from induced pluripotent stem cells in terms of origin, differentiation ability, and epigenetic status.[2,8]

Several advances in research have been made by using mouse ES cells. Furthermore, primate ES cell lines have been established from rhesus monkeys (*Macaca mulatta*),[24] common marmosets (*Callithrix jacchus*),[25] cynomolgus monkeys (*M. fascicularis*),[20] and African green monkeys (*Chlorocebus aethiops*).[19] Mouse and other mammalian ES cells differ markedly in their responses to the signaling pathways that support self-renewal.[8,28] Mouse ES cells require leukemia inhibitory factor (LIF)–STAT3 signaling.[14] In contrast, primate ES cells do not respond to LIF. Fibroblast growth factor 2 (FGF2) appears to be the most upstream self-renewal factor in primate ES cells. FGF2 also exerts its effects through indirect mechanisms, such as the TGFβ–Activin–Nodal signaling pathway, in primate ES cells.[21] In addition to the biologic similarities between monkeys and humans, ES cells derived from cynomolgus monkeys or human blastocysts have extensive similarities that are not apparent in mouse ES cells.[8,14,21,28] Numerous monkey ES cell lines are now available, and cynomolgus monkeys are an efficient model for developing strategies to investigate the efficacy of ES-cell–based medical treatments in humans.

Several growth factors and chemical compounds, including retinoic acid (RA),[4,9,13,22,26] FGF2,[9,10,16,22] epidermal growth factor,[9,22] SB431542,[1,4,10] dorsomorphin,[10,27] sonic hedgehog,[12,13,16,27,29] and noggin,[1,4,9,27] are essential for the differentiation and proliferation or maintenance of neural stem cells derived from primate ES cells. Of these factors, active RA signaling suppresses a mesodermal

Received: 27 Jul 2013. Revision requested: 04 Sep 2013. Accepted: 21 Sep 2013.
[1]Tsukuba Primate Research Center, National Institute of Biomedical Innovation, Tsukuba, Ibaraki, Japan; [2]Graduate School of Comprehensive Human Sciences, University of Tsukuba, Tsukuba, Ibaraki, Japan; [3]Institute for Frontier Medical Sciences, Kyoto University, Kyoto, Japan; [4]Institute for Integrated Cell-Material Sciences, Kyoto University, Kyoto, Japan; [5]RIKEN BioResource Center, Tsukuba, Ibaraki, Japan; [6]Center for Disease Biology and Integrative Medicine, Graduate School of Medicine, University of Tokyo, Bunkyo-ku, Tokyo, Japan.
[*]Corresponding author. Email: sankai@nibio.go.jp

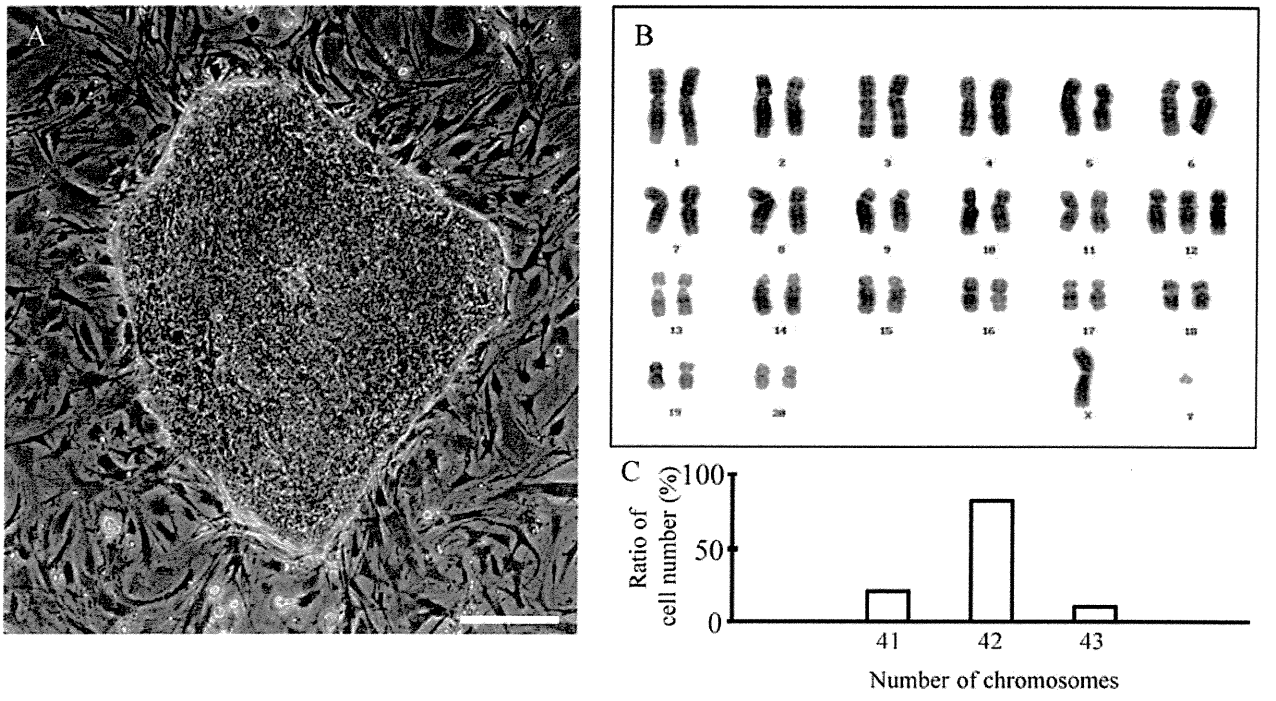

Figure 1. Established FGF2 low-dose–dependent Fld-ES cells and their karyotype analysis. (A) The colony was flat and had the features of a primate ES cell colony. (B) The 18 generations of Fld-ES cells. The chromosome number was normal (42). The sex chromosome was XY. (C) About 80% of cells had a normal chromosome number. Scale bar, 100 μm.

Table 1. ALP activity and evaluation of undifferentiation markers in Fld-ES cells

	FGF2 added	No FGF2 added		
Marker	Before passage	Passage 1	Passage 10	Passage 20
ALP	+	+	+	+
SSEA-1	−	−	−	−
SSEA-3	−	−	−	−
SSEA-4	+	+	+	+
TRA-1-60	+	+	+	+
TRA-1-81	+	+	+	+
Formation of EB	+	+	+	+

* P, passage numbers.

fate by inhibiting Wnt and Nodal signaling pathways during in vitro culture and leads to neuroectoderm differentiation in ES cells.[4,13,26] RA is an indispensable factor for the specialization to neural cells. FGF2 is important during nervous system development,[12] and FGF2 and RA both are believed to influence the differentiation to neural cells. The current study was done to clarify the mechanism of RA and FGF2 in the induction of differentiation along the neural lineage.

We recently established a monkey ES cell line that does not need FGF2 supplementation for maintenance of the undifferentiated state. This ES cell line allowed us to study the role of differentiation to neural cells with RA and enabled us to compare ES cell differentiation in the context of supplementation with RA or FGF2 in culture. To this end, we established a novel cynomolgus monkey cell line derived from ES cells and maintained it in an undifferentiated state in the absence of FGF2 supplementation.

Materials and Methods

Animals. Mature cynomolgus monkeys (*Macaca fascicularis*) are maintained in our facility according to guidelines set by the National Institute of Biomedical Innovation for the care, use, and biohazard countermeasures of laboratory animals. This study was approved by the institutional Animal Welfare and Animal Care Committee.

Derivation and culture of an FGF2 low-dose-dependent (Fld-) ES cell line. Procedures for the development of embryos and the establishment of ES cells from blastocysts that were developed in vitro were described previously.[28,29] Briefly, prominent inner cell masses derived from blastocysts of cynomolgus monkeys were cultured with mitomycin C-treated mouse embryonic fibroblast cell monolayers at a concentration of 4×10^4 cells/cm^2 on gelatin-coated dishes in embryonic stem cell medium (Dulbecco modified Eagle medium–Ham F12 nutrient mixture [1:1; Sigma, St Louis, MO] supplemented with 20% Knockout serum replacement [Invitrogen, Carlsbad, CA], 1 mM GlutaMax [Invitrogen], 1% nonessential amino acids [Invitrogen]) containing 4 ng/mL human recombinant basic FGF (FGF2; Wako Pure Chemical Industries, Osaka, Japan), 10 ng/mL human recombinant LIF (Merck Millipore, Billerica, MA), and 0.1 mM β-mercaptoethanol (Sigma). ES-like cell colonies were kept stable in culture with FGF2, human LIF, and β-mercaptoethanol for a total of 10 passages. Next, we transferred the ES-like cell colonies to modified ES cell medium without FGF2, human

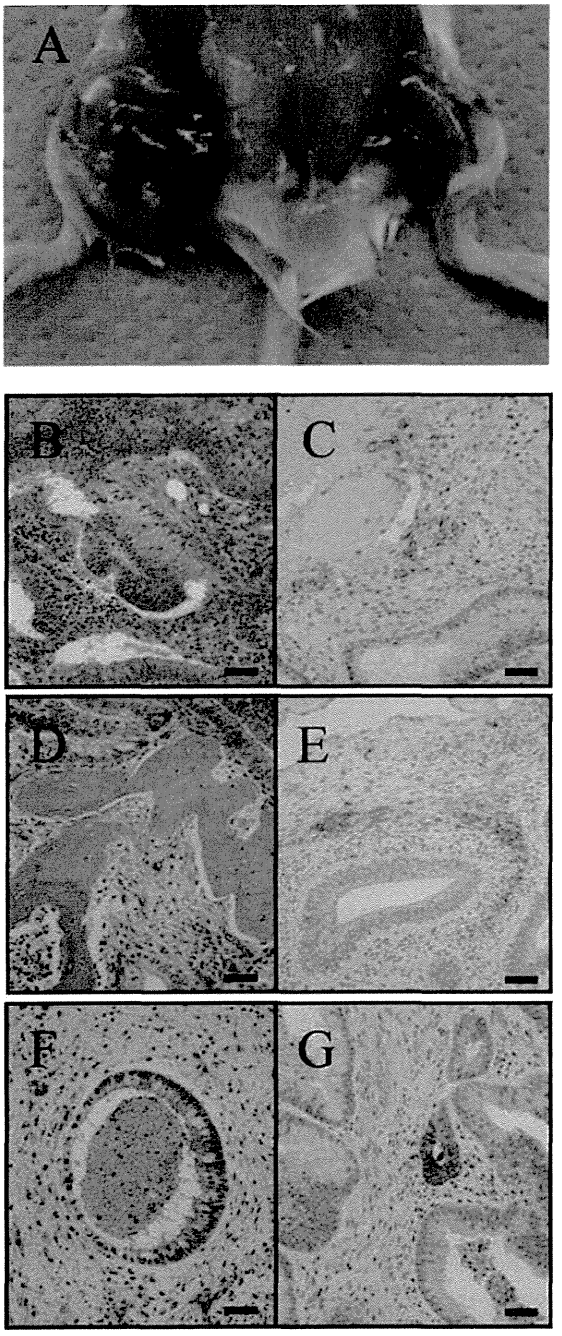

Figure 2. Teratoma formation from Fld-ES cells transplanted into immunodeficient mice (NOD/SCID). (A) The teratomas that formed from a small cluster of ES cells were transferred into the right hindleg muscle of NOD/SCID mice. (B–G) In vivo analysis of the multipotency of Fld-ES cells by histologic (left panel) and immunohistochemical (right panel) methods. Various tissues of the 3 germ-layer origins—neural tissue (B, ectoderm), bone (D, mesoderm), and gland (F, endoderm)— are identified. (C) The ectodermal marker is neuron-specific enolase. (E) The mesodermal marker is smooth-muscle actin. (G) The endodermal marker is α-fetoprotein. Scale bars, 100 μm.

LIF, or β-mercaptoethanol, thus creating the first generation of the FGF2 low-dose-dependent cell line (that is, Fld-ES line). The medium was changed daily, and ES-like cell colonies that proliferated were split every 7 d, either manually or by disaggregation in collagenase and replating of collected cells onto dishes with fresh feeder layers.

ES cells that had been maintained in culture without FGF2, human LIF and β-mercaptoethanol for 15 to 20 passages were karyotyped as previously described at the International Council for Laboratory Animal Science Monitoring Center (Kanagawa, Japan) or the Chromosome Science Lab (Hokkaido, Japan). Chromosome spreads were Giemsa-banded, photographed, and sorted.

For pluripotency analysis, embryoid bodies (EB) and teratomas were prepared from ES cells. EB were developed in a suspension culture from collagenase-treated ES cells grown in suspension. After 2 wk, EB were transferred to 6-cm dishes coated with 0.1% gelatin in modified ES cell medium for attachment culture. For the evaluation of teratoma formation, small-cluster subcultured ES cells from a 6-cm dish were transferred into the right hindleg muscles of 2 NOD/SCID mice. The tumors that formed were fixed with 4% paraformaldehyde in PBS, embedded in paraffin, and sectioned for histologic and immunohistochemical analysis. Histologic analysis was done with hematoxylin and eosin staining. Immunohistochemical analysis was done by visualizing the localization of primary antibodies by using horseradish-peroxidase–labeled secondary antibody and diaminobenzidine. Primary antibodies were α-smooth muscle actin (dilution, 1:100; Dako, Glostrup, Denmark), synaptophysin (1:200; Dako) and α-fetoprotein (1:1000; Dako).

EB formation and attachment assay. The percentage of attached EB that developed from Fld-ES cells was determined by microscopic observation. EB of 300 to 500 μm and 500 to 700 μm in diameter were counted and separated into 6-cm dishes coated with 0.1% gelatin. After 3 d of culture, attachment was confirmed, and the 2 size groups were compared.

Effect of RA dose on EB attachment and differentiation. To induce the neural differentiation of Fld-ES cells, we assessed various doses of RA (all-trans-retinoic acid, catalog no. R2625, Sigma Aldrich) from 0.5 μM to 100 μM in the medium. After 3 d, we counted the attached EB, and after 10 d we counted the neural-like cell colonies from the outgrowth of the cultured EB and recorded the dose-dependent effect of RA.

Induction of neural differentiation from Fld-ES cells. To assess neural differentiation, we used Fld-ES and CMK6, a stable cynomolgus monkey ES cell line.[5,20] CMK6 cells were cultured on mitomycin-C-treated mouse embryonic fibroblast monolayers at a concentration of 4×10^4 cells/cm^2 on gelatin-coated dishes in ES cell medium. Before the Fld-ES and CMK6 ES cells differentiated into neural cells, we divided them into 3 groups according to the differentiation-inducing factors used. Briefly, EB that formed from Fld-ES and CMK6 cells after 3 d of passage were transferred into 6-cm dishes coated with 0.1% gelatin, and attachment culture was initiated in the 3 groups. To group A (Fld-ES cells) and group C (CMK6 cells), we added only 1 μM RA. To group B (Fld-ES cells), we added 1 μM RA and 10 ng/mL FGF2. After 3 d, we confirmed the attachment of EB to the dishes in each group.

The attachment cultures of EB were maintained in fresh medium that was changed every 3 d. After 30 d of attachment